

Time series analysis methods

Some alternatives

Jaan Pelt

Tartu Observatory

Space Climate School

March 30 – April 3, 2016

Levi, Finnish Lapland



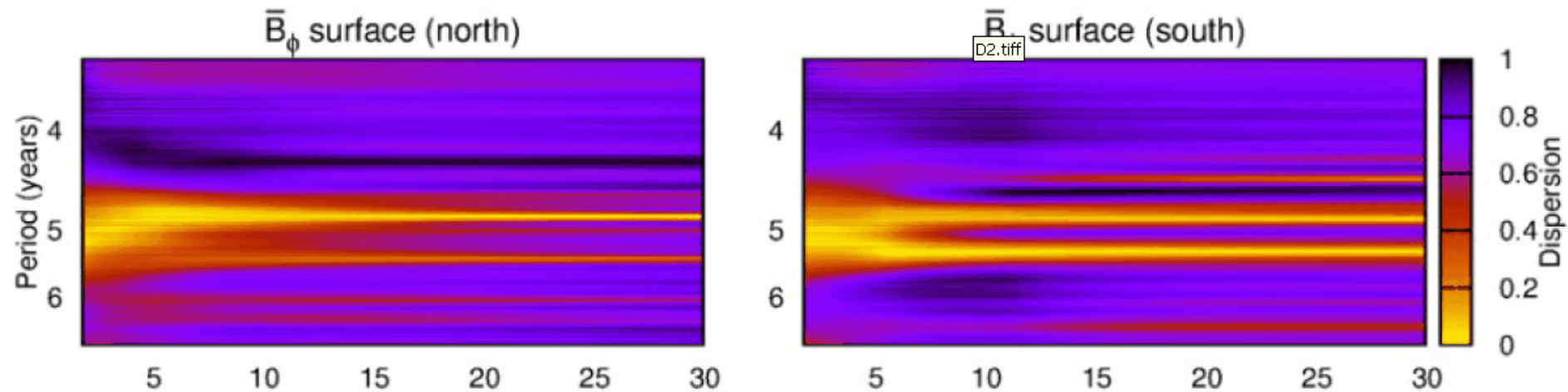
From harmonics to cycles

- Harmonics
- Periods
- Multiperiodicity
- Cyclicity

Plan

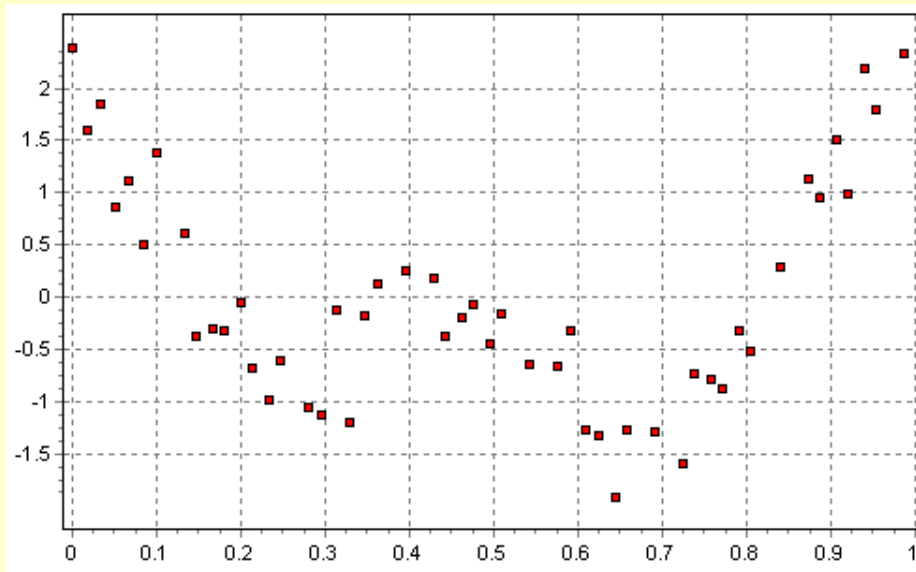
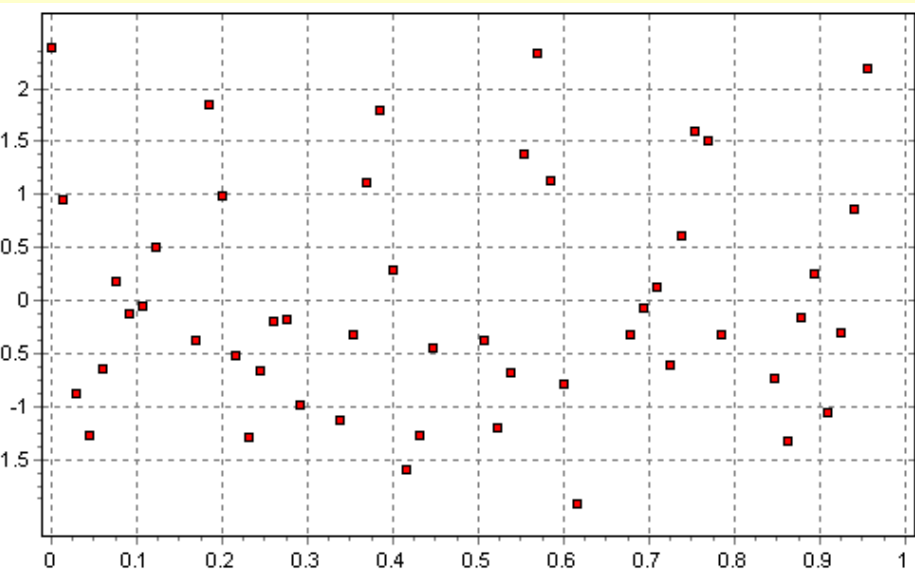
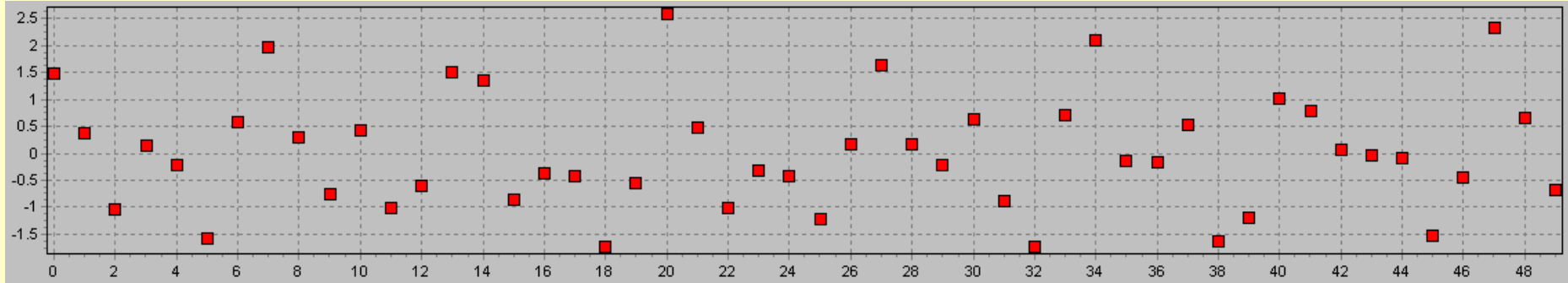
- What is D^2 method?
- What is CF method?
- What is FDC method?.

What is D^2 method?



- D^2 analysis (correlating only phases over a certain coherence time, not over the full time span) reveals the *dominating "solar butterfly" –like period of roughly 5.35 years.*
- This is roughly 4 times shorter than the solar cycle, but if scaled back to solar time units, the simulation length would be roughly 2 millennia.

Phase-process diagram (folding)



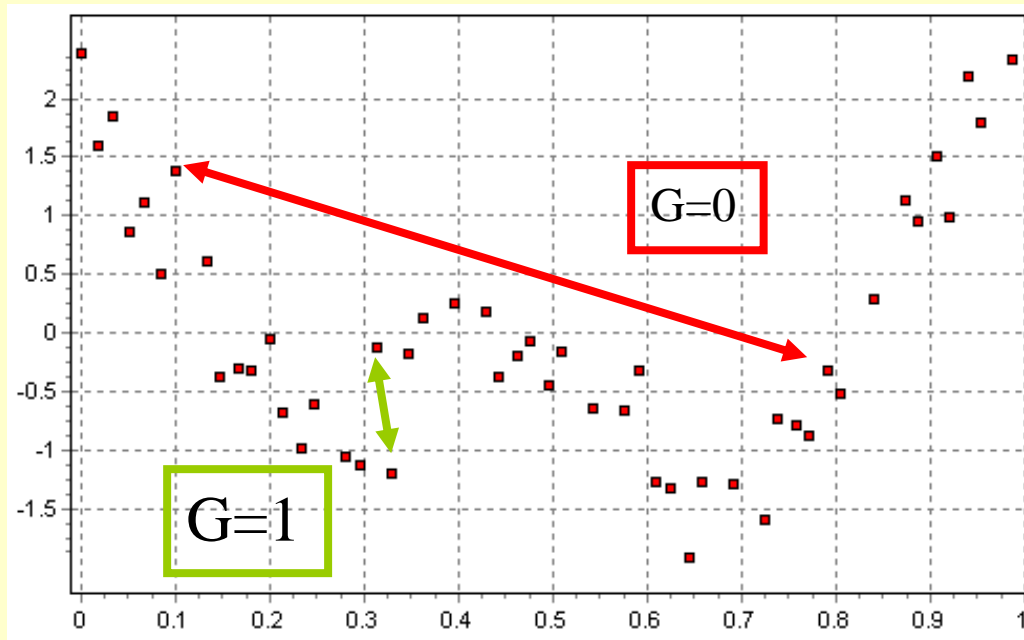
$$t_i, f(t_i), i = 1, 2, \dots, N$$

$$\varphi_P(t_i) = \text{Frac}(t_i P^{-1})$$

$$D^2(\nu) = \frac{\sum_{i=1}^{N-1} \sum_{j=i+1}^N G(t_i, t_j, \nu) [f(t_i) - f(t_j)]^2}{2 \sum_{i=1}^{N-1} \sum_{j=i+1}^N G(t_i, t_j, \nu)}$$

Weights G are larger than zero when phases of two points in pair are similar, or:

$$t_i - t_j \approx \frac{k}{\nu}, k = 0, \pm 1, \pm 2, \dots,$$



Smother periodograms

$$D^2(\nu) = \frac{\sum_{i=1}^{N-1} \sum_{j=i+1}^N G^*(t_i, t_j, \nu) [f(t_i) - f(t_j)]^2}{2 \sum_{i=1}^{N-1} \sum_{j=i+1}^N G^*(t_i, t_j, \nu)}$$

$$G^*(t_i, t_j, \nu) = G(t_i, t_j, \nu) W(t_i, t_j)$$

$$W(t_i, t_j) = \begin{cases} 1, & |t_i - t_j| \leq t_{\max} \\ 0, & \text{otherwise,} \end{cases}$$

How to compute?

$$t_i - t_j \approx k\delta t, \text{ for some } k$$

$$D^2(\nu) = \frac{\sum_{i=1}^{N-1} \sum_{j=i+1}^N G(t_i, t_j, \nu) [f(t_i) - f(t_j)]^2}{2 \sum_{i=1}^{N-1} \sum_{j=i+1}^N G(t_i, t_j, \nu)}$$

$$C_k = \sum_{t_i - t_j \approx k\delta t} [f(t_i) - f(t_j)]^2$$

$$S_k = \sum_{t_i - t_j \approx k\delta t} 1$$

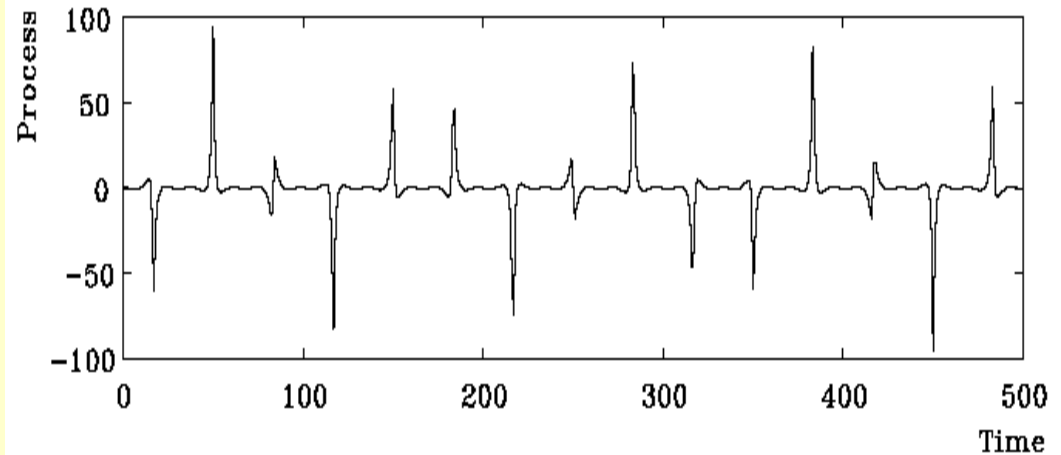
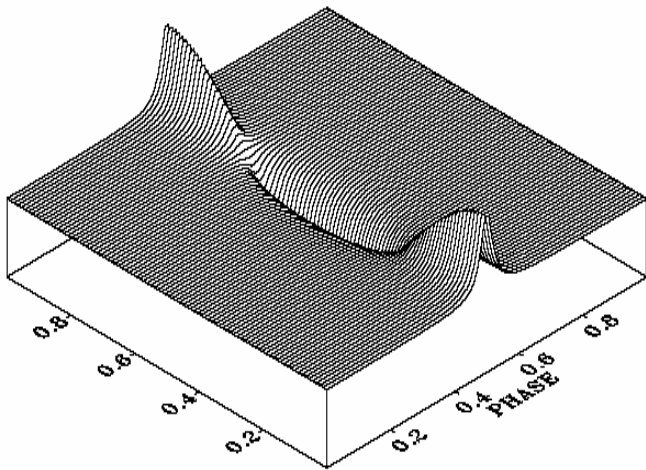
$$G(t_i, t_j, \nu) = d((t_i - t_j)\nu) \approx d(k\delta t\nu)$$

$$D^2(\nu) = \frac{\sum_{k=0}^K d(k\delta t\nu) C_k}{2 \sum_{k=0}^K d(k\delta t\nu) S_k}$$

$$d(k\delta t\nu) = \sum_{r=0}^{\infty} d_r \cos(2\pi r k\delta t\nu)$$

Multiperiodic oscillations

$$f(t) = \sum_{k_1=-\infty}^{\infty} \dots \sum_{k_R=-\infty}^{\infty} \left(a_{k_1, \dots, k_R} \cos\left(2\pi \sum_{r=1}^R k_r \bar{\nu}_r t\right) + b_{k_1, \dots, k_R} \sin\left(2\pi \sum_{r=1}^R k_r \bar{\nu}_r t\right) \right) + \varepsilon(t).$$



Phase dispersion for multiperiodic processes

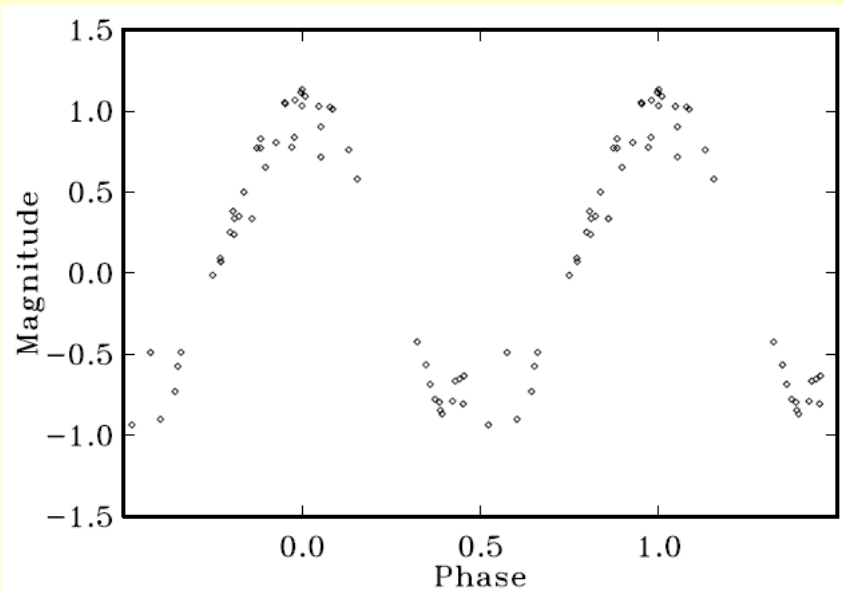
$$\frac{\sum_{i=1}^{N-1} \sum_{j=i+1}^N G(t_i, t_j, \nu_1, \nu_2) [f(t_i) - f(t_j)]^2}{2 \sum_{i=1}^{N-1} \sum_{j=i+1}^N G(t_i, t_j, \nu_1, \nu_2)}$$

An example

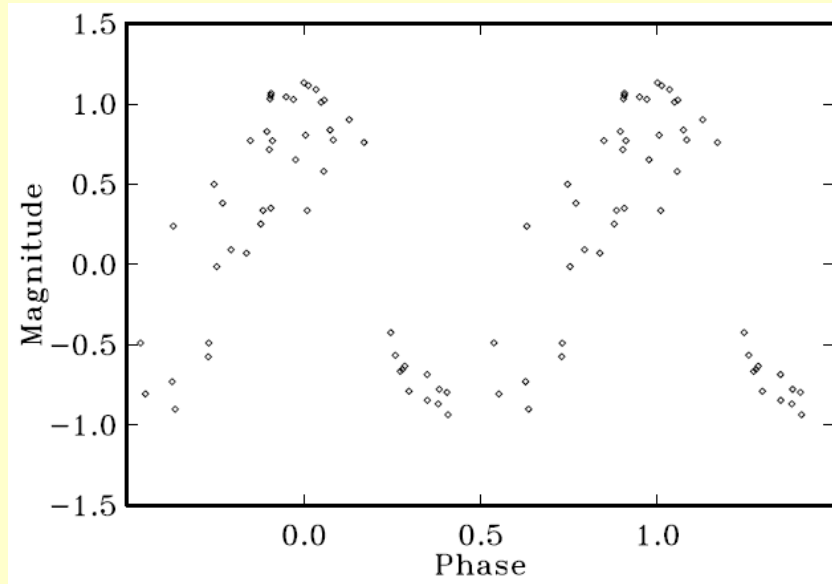
$$f(t) = 0.55073 \cos(2\pi t/0.53289 + 0.09111) + \\ + 0.58717 \cos(2\pi t/7.83453 + 0.91564).$$



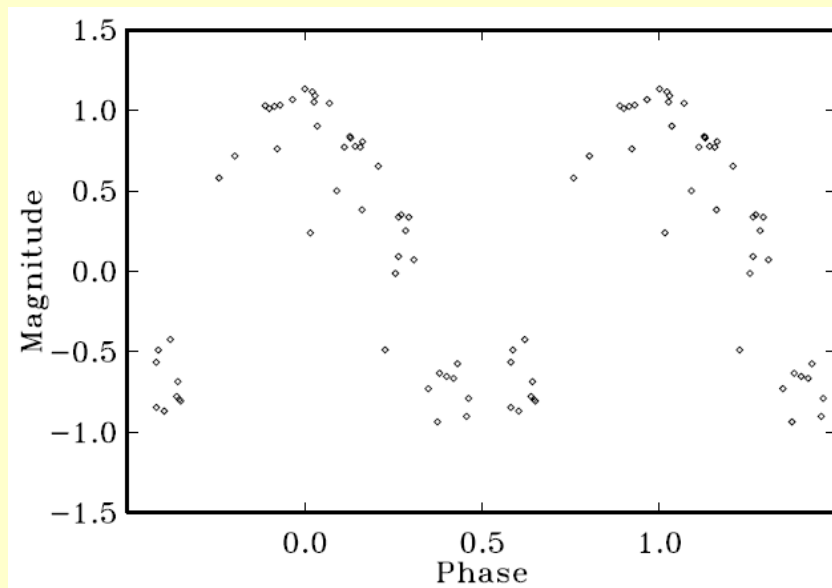
Why?



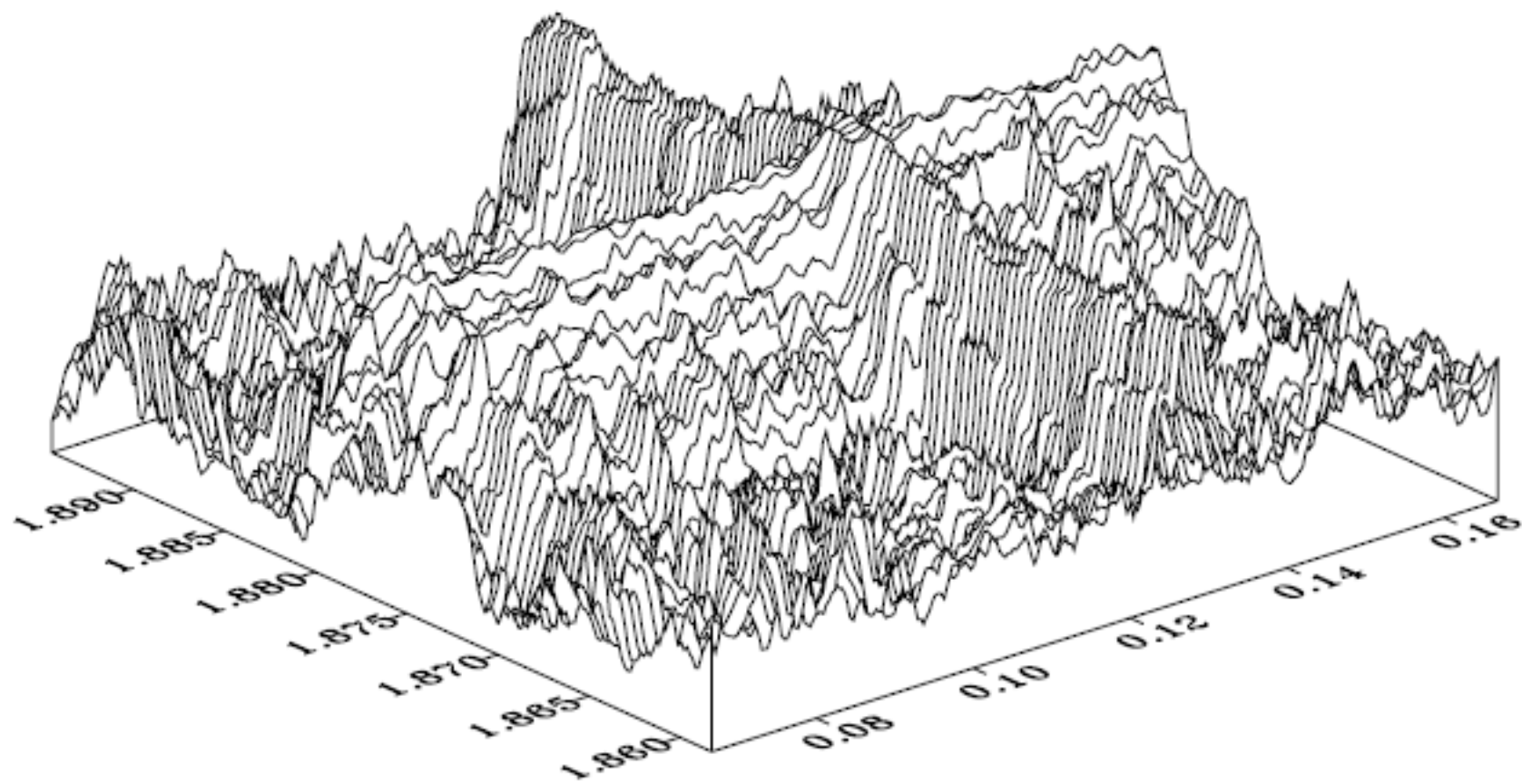
deepest peak in spectrum $P = 1.143455$



first real period $P = 0.5328956$

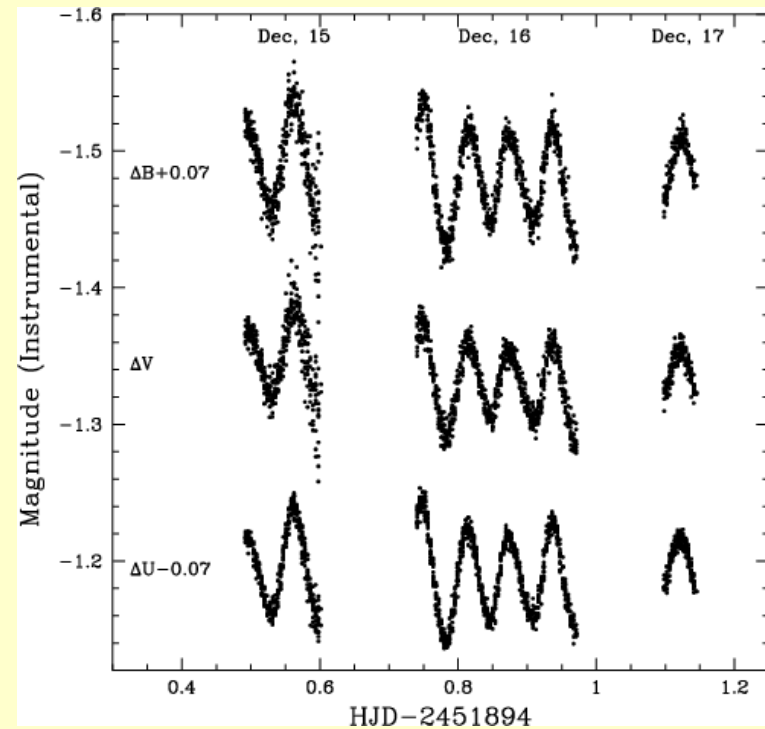


second real period $P = 7.8345346$



Two-dimensional "power spectrum" $1 - D(\nu_1, \nu_2)$

Multichannel search



$$t_{ij} = |t_i - t_j|,$$

$$w_{ij}^c = \frac{1}{\sigma^c(t_i)^2 + \sigma^c(t_j)^2} = \frac{w_i^c \cdot w_j^c}{w_i^c + w_j^c},$$

$$y_{ij}^c = w_{ij}^c \cdot |y_i^c - y_j^c|^2.$$

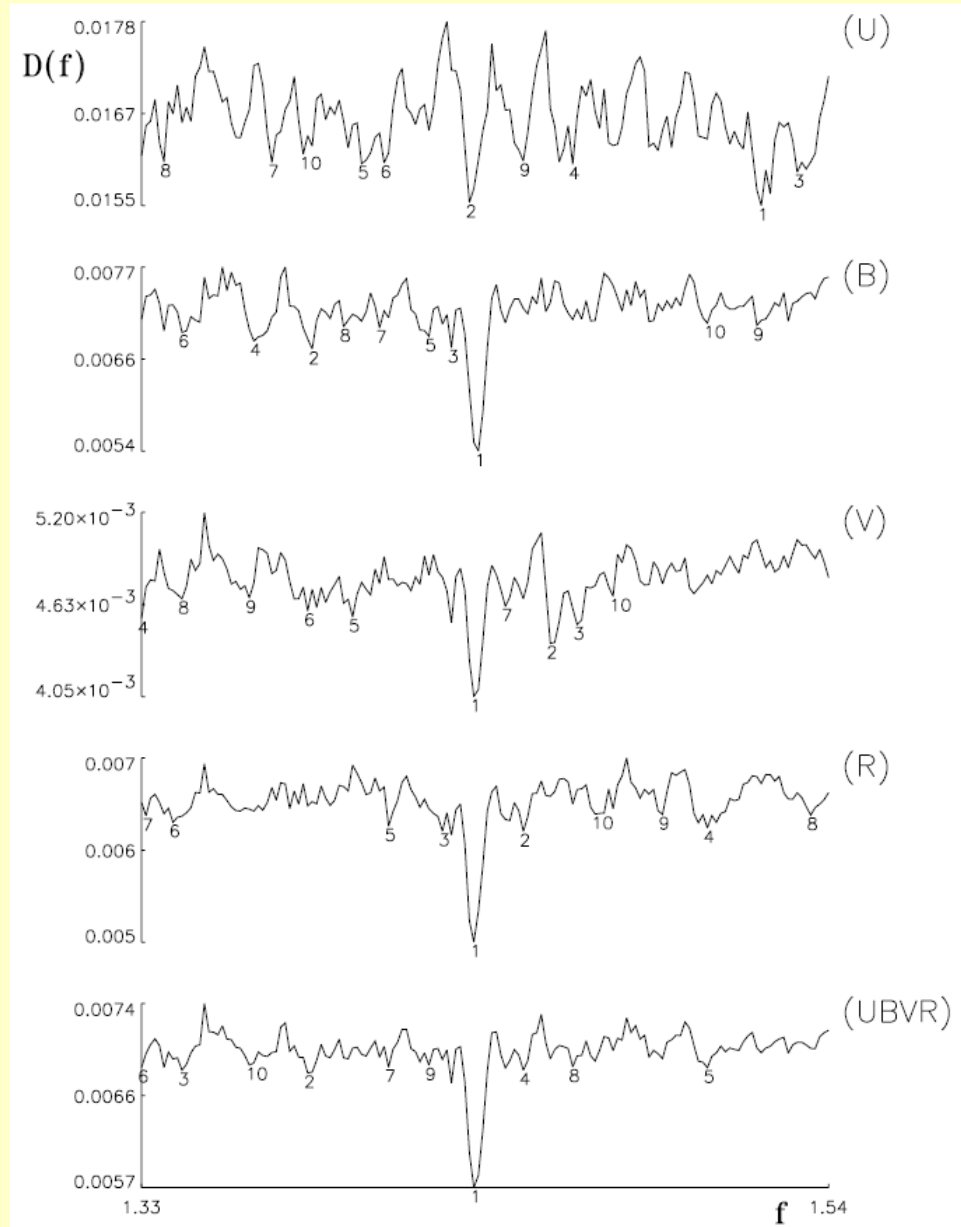
Many channels in LSQ format

Dispersions in separate channels

$$WRSS^c(P) = \sum_{i=1}^N w_i^c [y_i^c - M(t_i, \beta^c(P))]^2$$

Total dispersion

$$WRSS(P) = \sum_{c=1}^C WRSS^c(P)$$



Total dispersion

$$D(P) = \frac{\sum_{c=1}^C \sum_{i=1}^{N-1} \sum_{j=i+1}^N g(t_{ij}, P) L(t_{ij}) y_{ij}^c}{\sum_{c=1}^C \sum_{i=1}^{N-1} \sum_{j=i+1}^N g(t_{ij}, P) L(t_{ij}) w_{ij}^c}.$$

Phases

$$\phi_{ij}(P) = \text{Frac} \frac{t_i - t_j}{P}.$$

must be near by

$$g(t_{ij}, P) = \begin{cases} 1, & \phi_{ij}(P) \leq \tau \quad \text{or} \\ & \phi_{ij}(P) > 1 - \tau \\ 0, & \text{otherwise.} \end{cases}$$

Resolution
can be
controlled

$$L(t_{ij}) = \begin{cases} 1, & D_{\min} \leq |t_i - t_j| < D_{\max} \\ 0, & \text{otherwise.} \end{cases}$$

$$D^2(P, \Delta t) = \frac{\sum_{i=1}^{N-1} \sum_{j=i+1}^N g(t_i, t_j, P, \Delta t) [f(t_i) - f(t_j)]^2}{2\sigma^2 \sum_{i=1}^{N-1} \sum_{j=i+1}^N g(t_i, t_j, P, \Delta t)}, \quad (\text{B.1})$$

where $f(t_i), i = 1, \dots, N$ is the input time series, σ^2 is its variance, $g(t_i, t_j, P, \Delta t)$ is the selection function, which is significantly greater than zero only when

$$t_j - t_i \approx kP, k = \pm 1, \pm 2, \dots \quad \text{and} \quad (\text{B.2})$$

$$|t_j - t_i| \lesssim \Delta t, \quad (\text{B.3})$$

where P is the trial period and Δt is the so-called coherence time, which is the measure of the width of the sliding time window wherein the data points are taken into account

$$g(t_i, t_j, P, \Delta t) = g_1(t_i, t_j, P) \cdot g_2(t_i, t_j, \Delta t), \quad (\text{B.4})$$

$$g_1(t_i, t_j, P) = \frac{1}{2} \left(\cos \left(2\pi \cdot \text{frac} \left(\frac{t_j - t_i}{P} \right) \right) + 1 \right), \quad (\text{B.5})$$

$$g_2(t_i, t_j, \Delta t) = \exp \left(-\ln 2 \left(\frac{t_j - t_i}{\Delta t} \right)^2 \right), \quad (\text{B.6})$$

where $\text{frac}((t_j - t_i)/P)$ removes the integer part of $(t_j - t_i)/P$.

Phase weighting and coherence weighting

$a = 0.0$

'thetapl.t.dat'

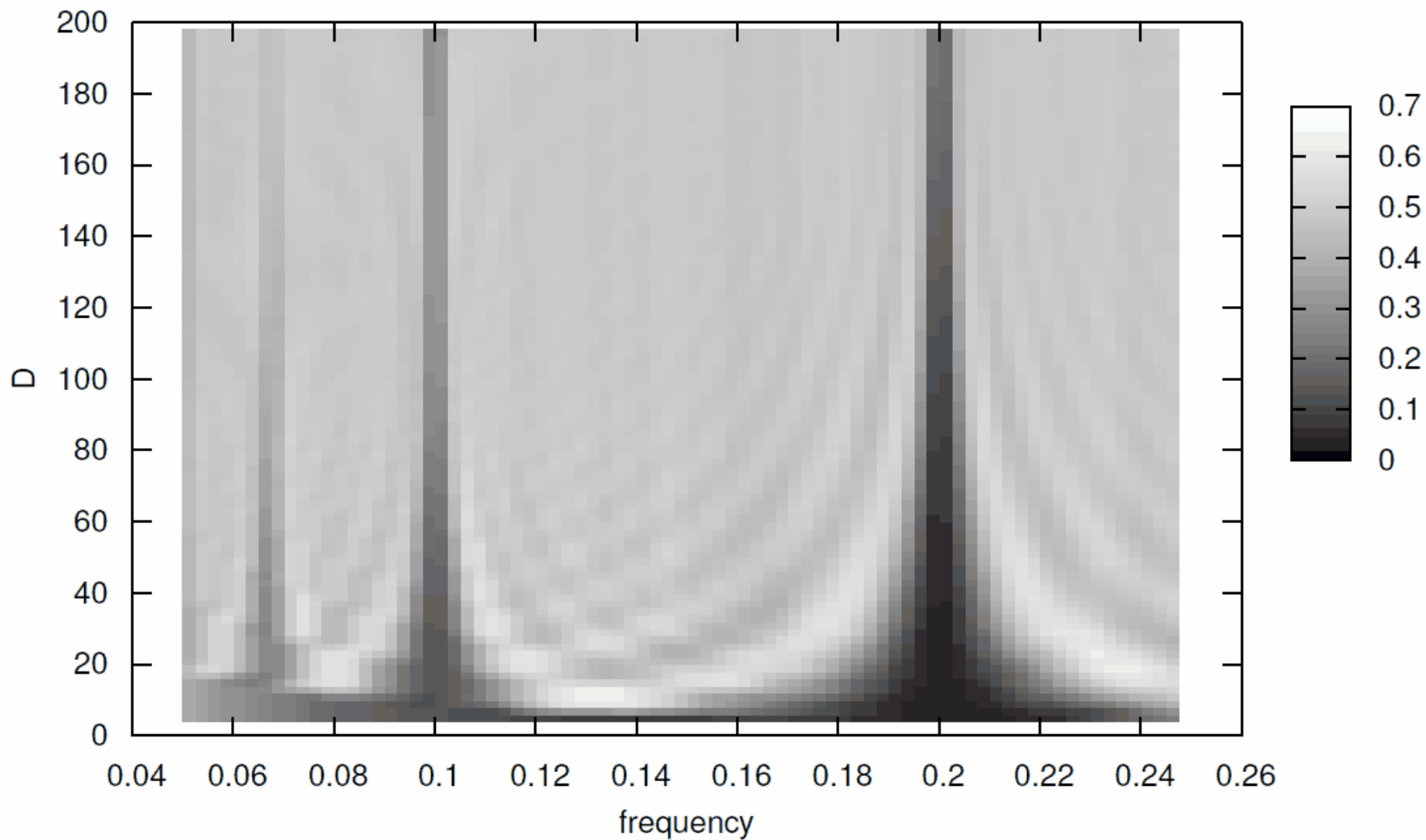


Figure 1: (ν, D) -spectrum for data with constant frequency

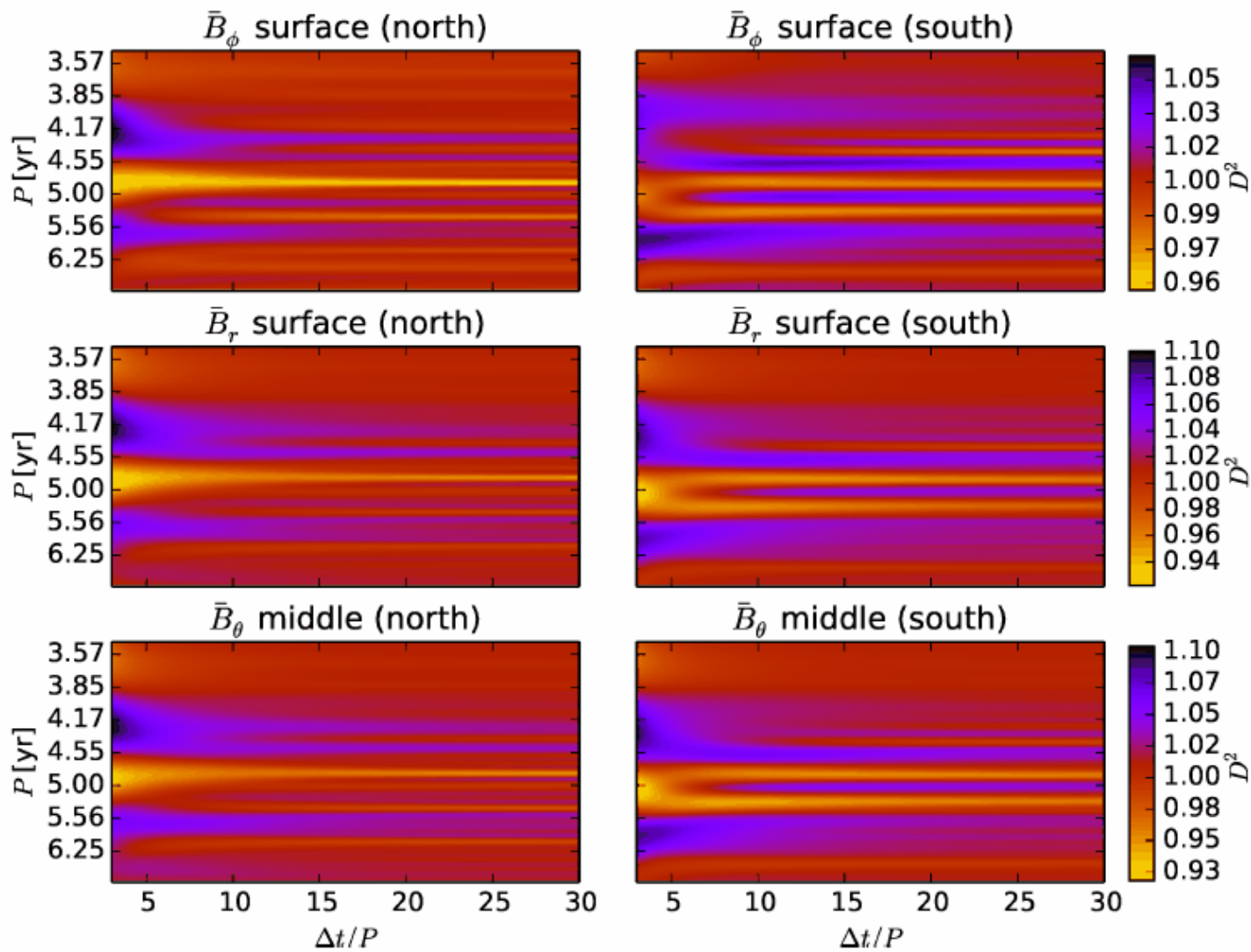
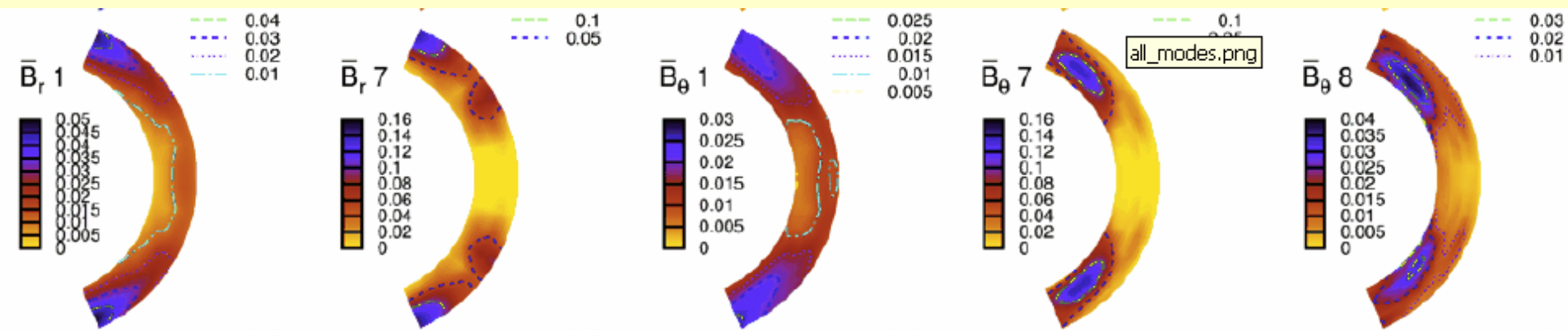


Fig. 6. Phase dispersion analysis results for the components of \bar{B} . The calculations were done for \bar{B}_ϕ at latitude $\pm 22^\circ$ and radius $0.94R_\odot$, for \bar{B}_r at latitude $\pm 66^\circ$ and radius $0.94R_\odot$, and for \bar{B}_θ at latitude $\pm 49^\circ$ and radius $0.82R_\odot$. Left (right) refers to the northern (southern) hemisphere.



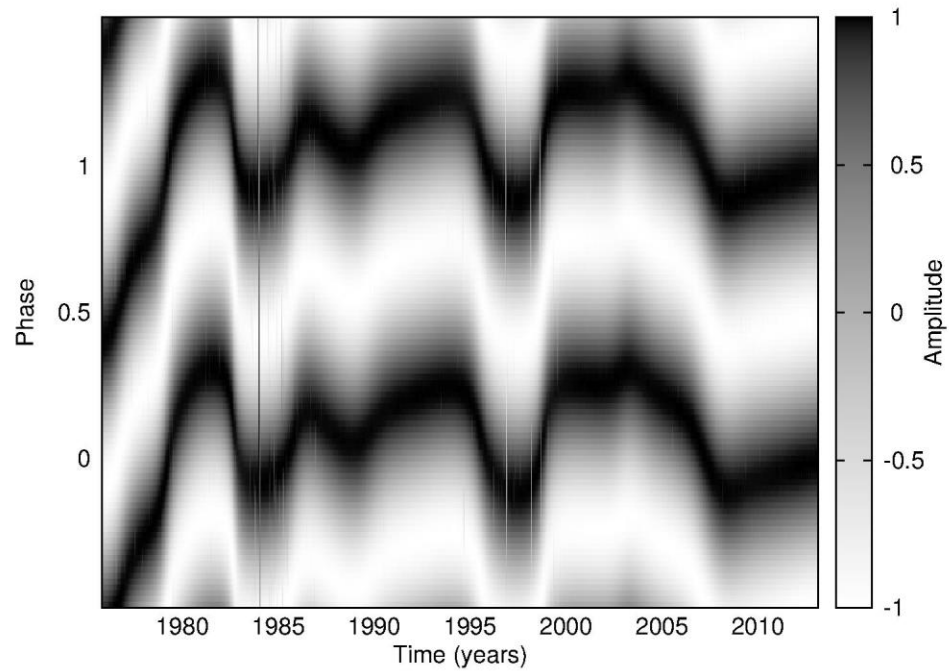
From photometric channels to N^2 or more time dependent pixels.

Distances need to be computed only once!

D² Summary

- D² method can be used for search of periods in irregularly spaced data
- It is usable also in context where periodicity is only approximate (process is cyclic)
- Method can be easily generalized for different geometries
- D² method allows to classify data curves in frequency and coherence terms

What is CF method?



Basic model

Model with single harmonic carrier:

$$f(t) = a(t) \cos(2\pi\nu_0 t) + b(t) \sin(2\pi\nu_0 t),$$

where ν_0 is so called *carrier frequency*.

More general waveform:

$$f(t) = \sum_{k=1}^K a_k(t) \cos(2\pi k\nu_0 t) + b_k(t) \sin(2\pi k\nu_0 t)$$

The coefficients themselves are modeled using harmonic expansions:

$$a_k(t) = \sum_l^L a_{kl}^{(a)} \cos(2\pi l \nu_m t) + b_{kl}^{(a)} \sin(2\pi l \nu_m t),$$

$$b_k(t) = \sum_l^L a_{kl}^{(b)} \cos(2\pi l \nu_m t) + b_{kl}^{(b)} \sin(2\pi l \nu_m t).$$

What to do with modulating curves?

For our special case (due to the theorem of Bedrosian) we can define *Hilbert transform* in the following way—if the original function is:

$$u(t) = a(t) \cos(2\pi f_0 t) + b(t) \sin(2\pi f_0 t),$$

then its Hilbert transformed image is:

$$v(t) = a(t) \sin(2\pi f_0 t) - b(t) \cos(2\pi f_0 t).$$

This is true when frequency domain support for $a(t), b(t)$ do not overlap with carrier frequency f_0 . The good news is, that (as we saw before) the pair of functions $u(t), v(t)$ allows us to define *instantaneous frequency, phase and amplitude* for the every time point of the model curve.

Instantaneous values

Amplitude:

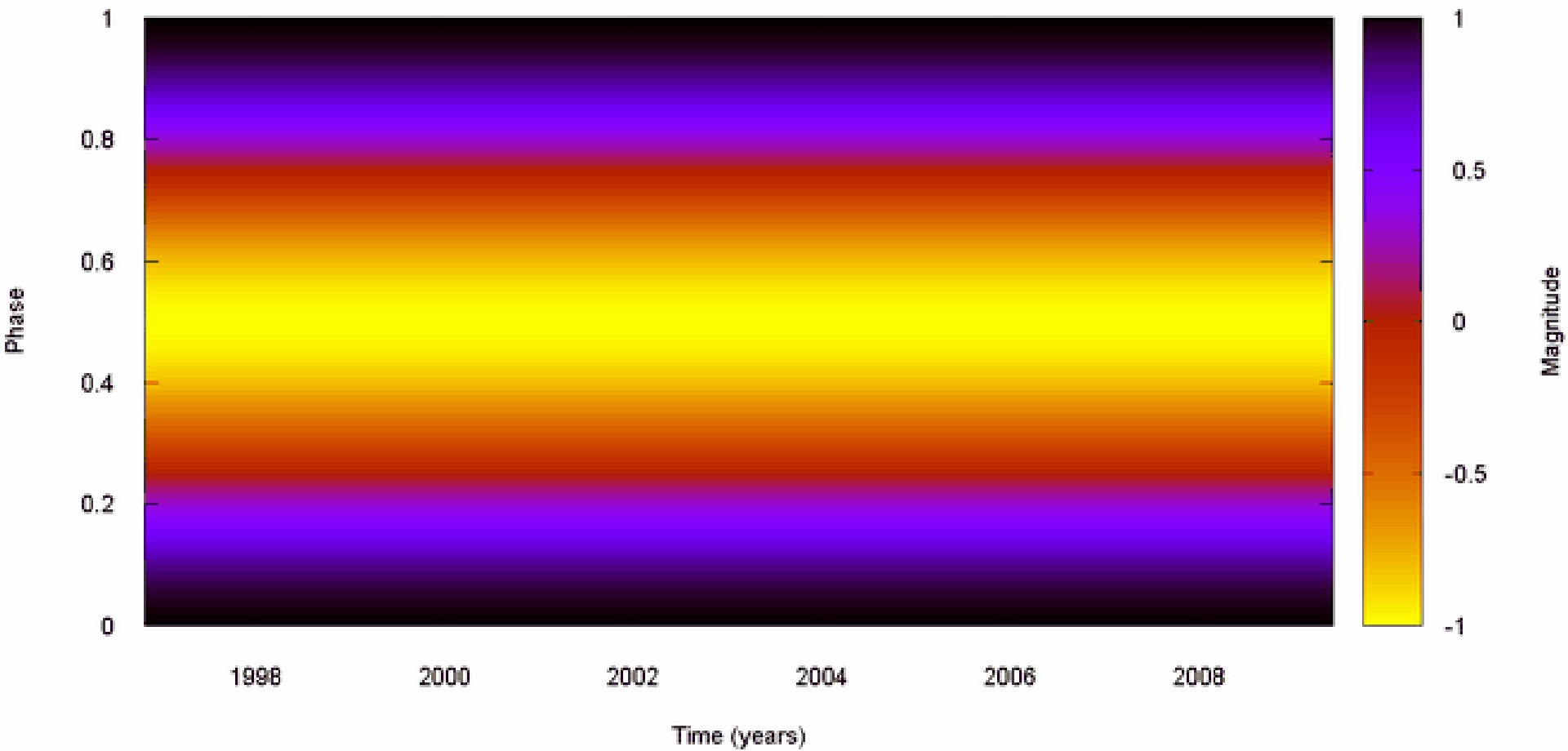
$$A(t) = \sqrt{u^2(t) + v^2(t)},$$

frequency:

$$\nu(t) = \frac{v'(t)u(t) - u'(t)v(t)}{u^2(t) + v^2(t)},$$

phase:

$$\phi(t) = \arctan\left(\frac{u(t)}{v(t)}\right).$$



Simple sinusoid

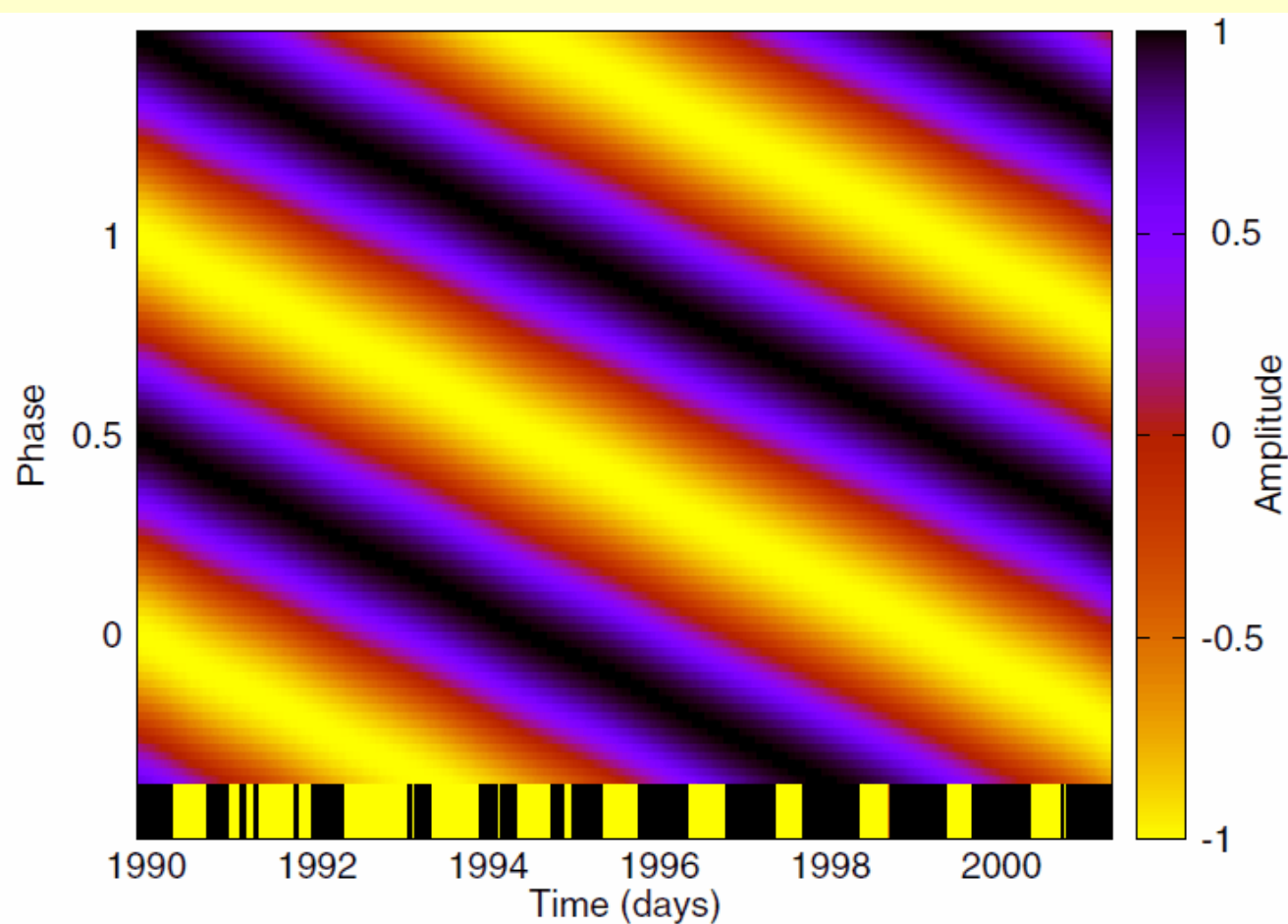


Fig. 4. Time-dependent phase diagram, i.e. the light curve amplitude profile over phase (y -axis) plotted as function of time (x -axis), for the mismatched carrier frequency example presented in Sect. 3.2. In this plot, a slightly too low carrier frequency of $\nu_0 = 0.148714$ is used, with $K = 1$ model and $L = 8$ modulation harmonics. Time points are obtained from real V -band photometric observations of LQ Hya; the bar-code in the bottom of the plot indicates when data has been available (black) and the gaps (bright). For visualization details see Sect. 2.6.

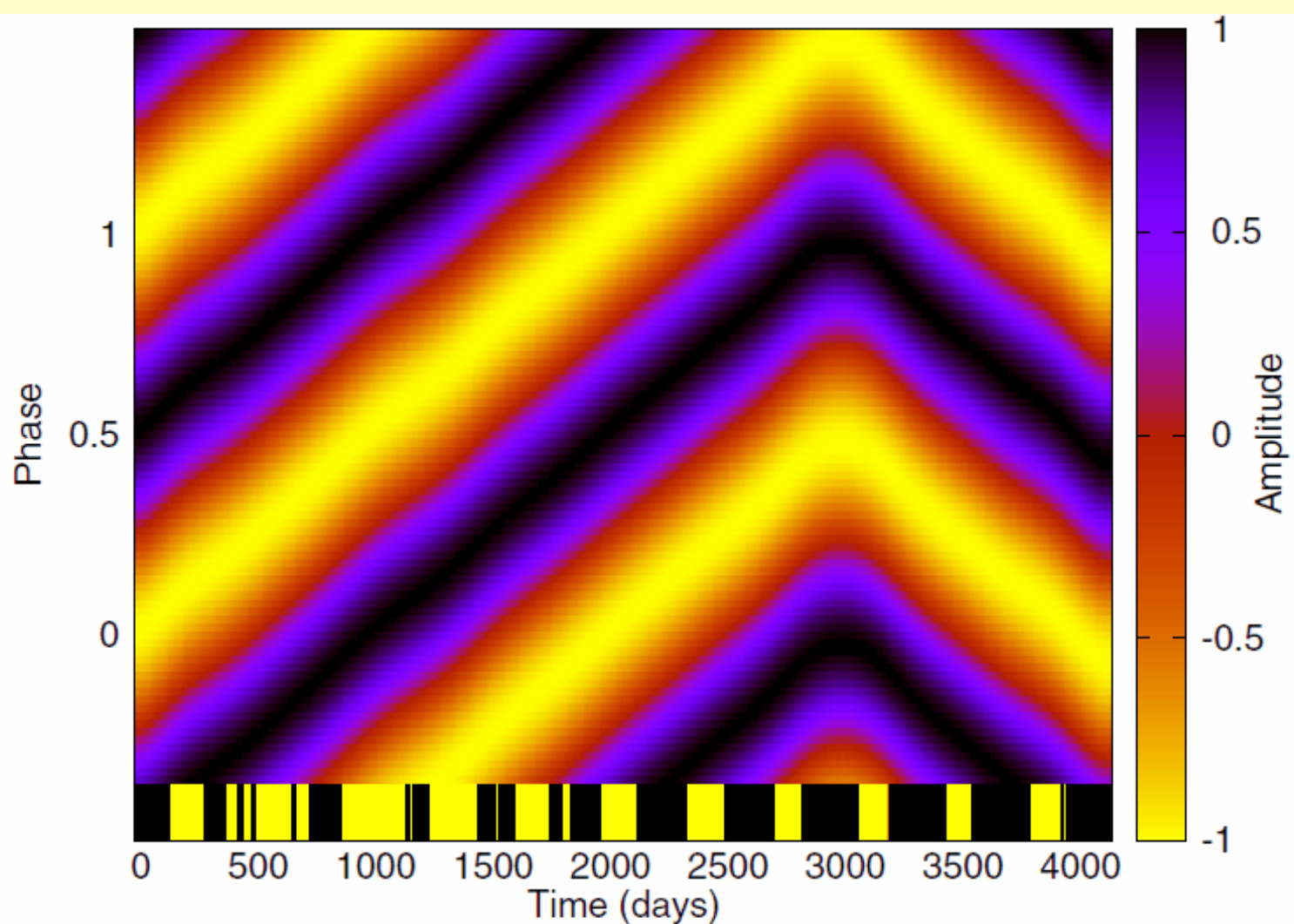


Fig. 7. The effect of an abrupt change in the period (Sect. 3.3) in the time-dependent phase diagram. The period before the jump is $P_1 = 6.747017$, and after it $P_2 = 6.7018004$. The used carrier is $P_0 = 6.724333$, the number of model harmonics, $K = 1$, and the number of modulation harmonics, $L = 8$.

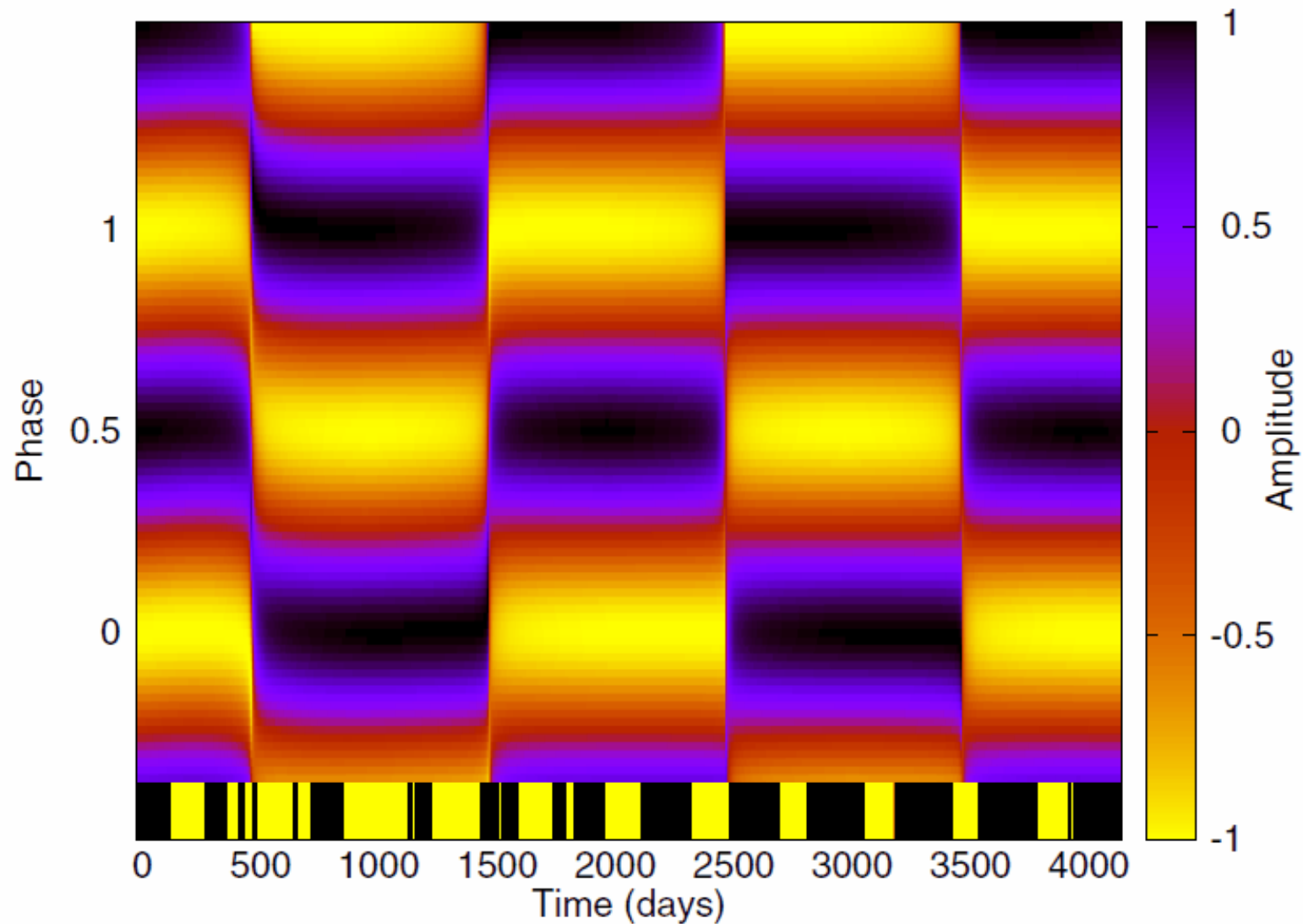


Fig. 9. The effect of two beating periods, $P_1 = 6.747017$ and $P_2 = 6.701800$, in the time-dependent phase diagram. The carrier used is $P_0 = 6.724333$, the number of model harmonics $K = 1$, and the number of modulation harmonics $L = 8$. See Sect. 3.4.

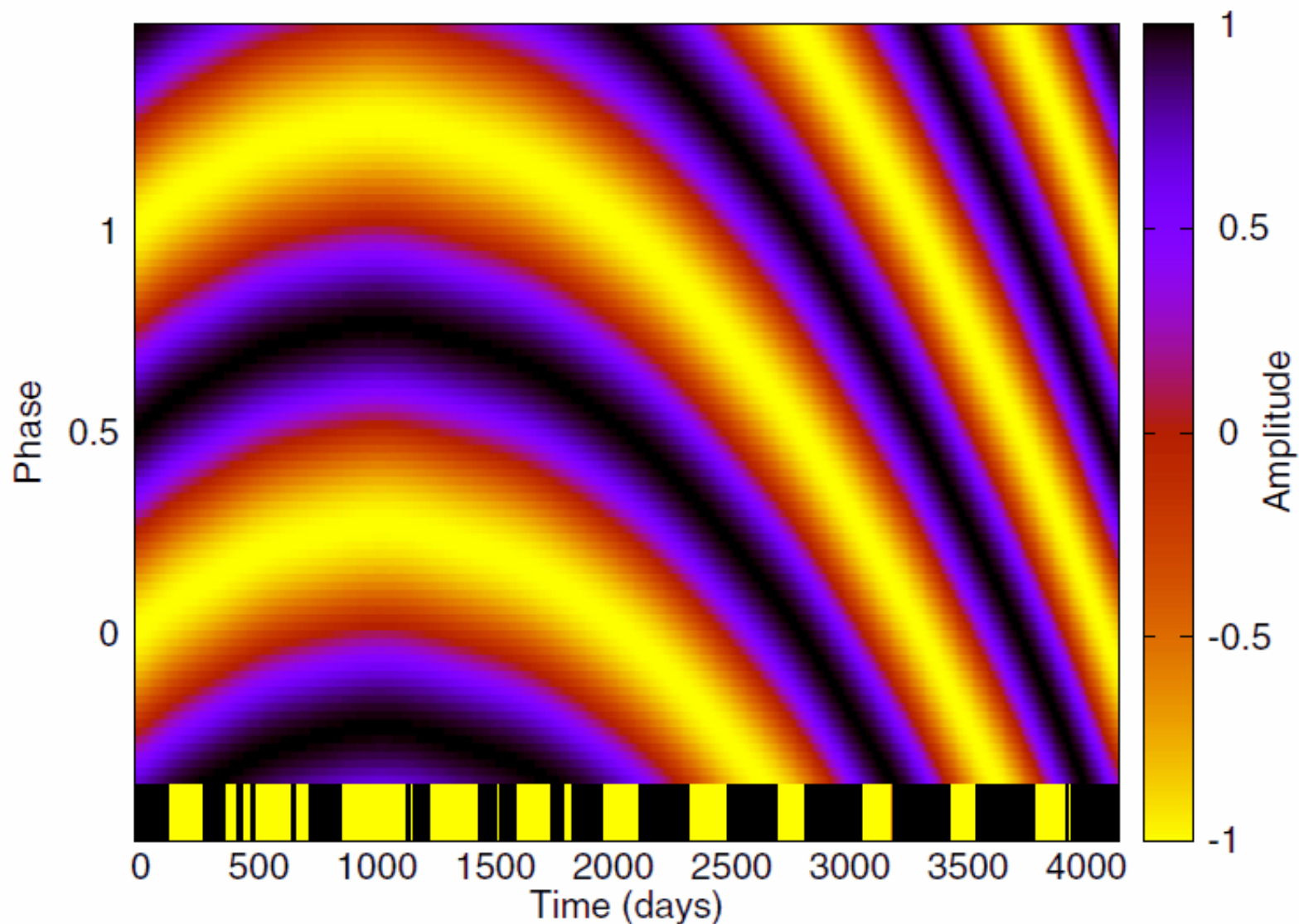
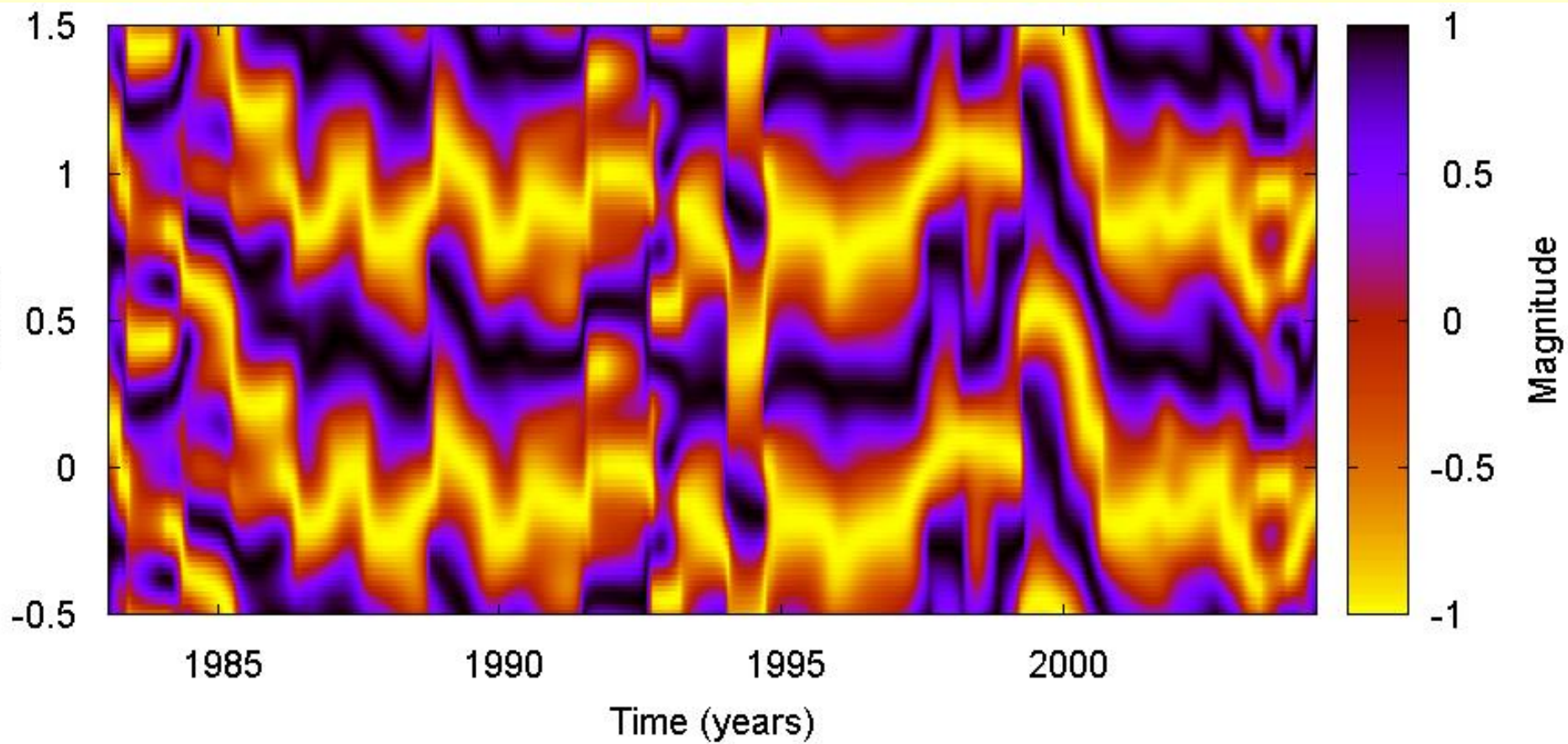
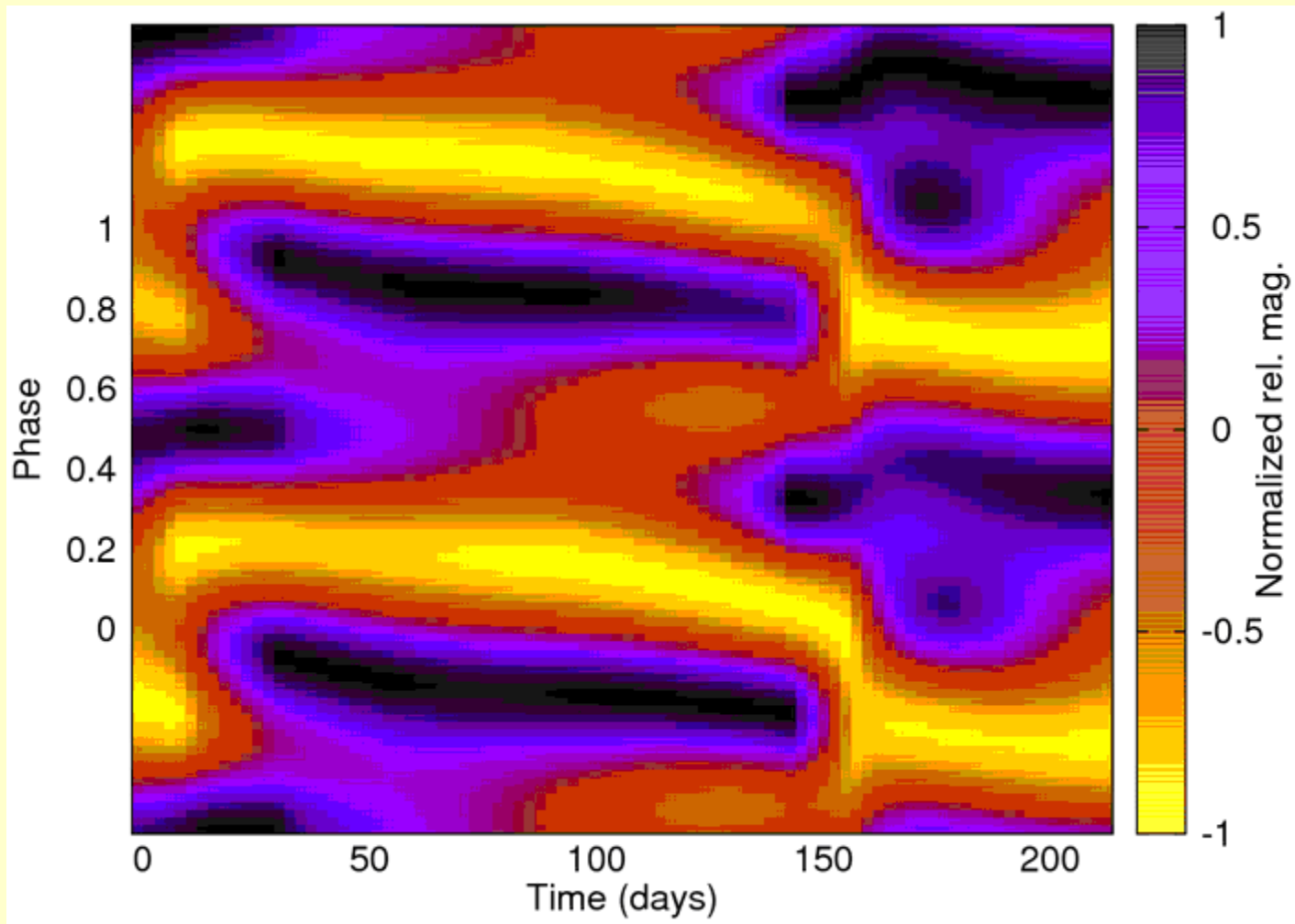


Fig. 12. The effect of a linear trend in frequency, as described in Sect. 3.5, in the time-dependent phase diagram. The used model parameters for the carrier fit read $\nu_0 = 0.148714$, $K = 1$, and $L = 8$.



FK Com

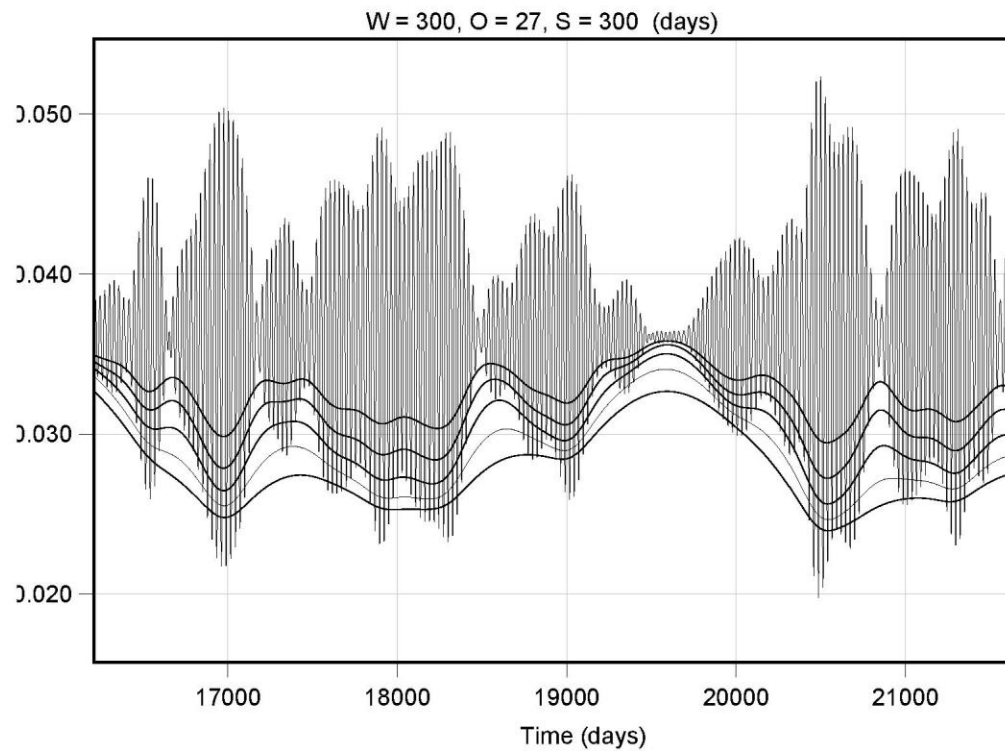


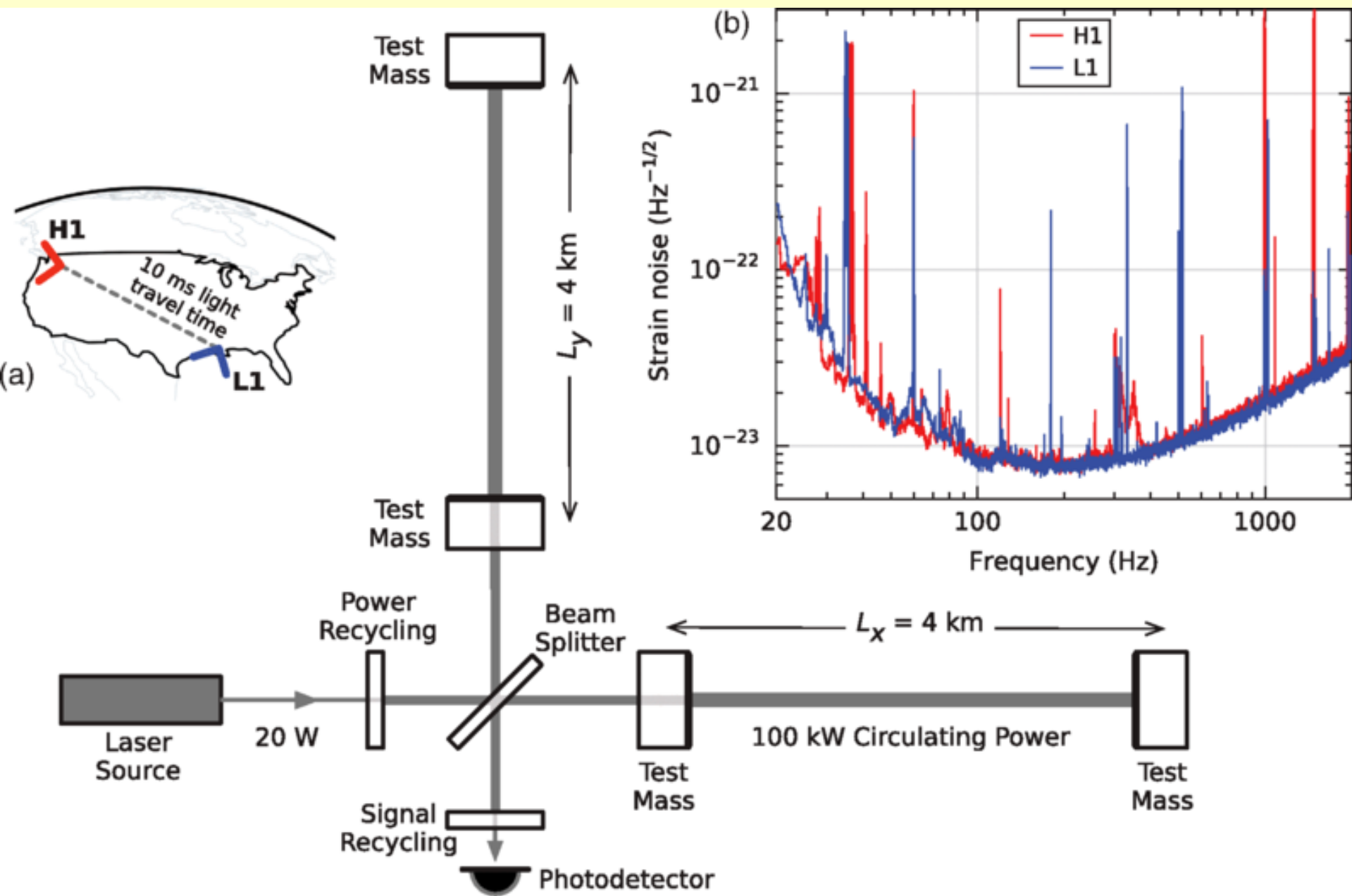
FK Com detail

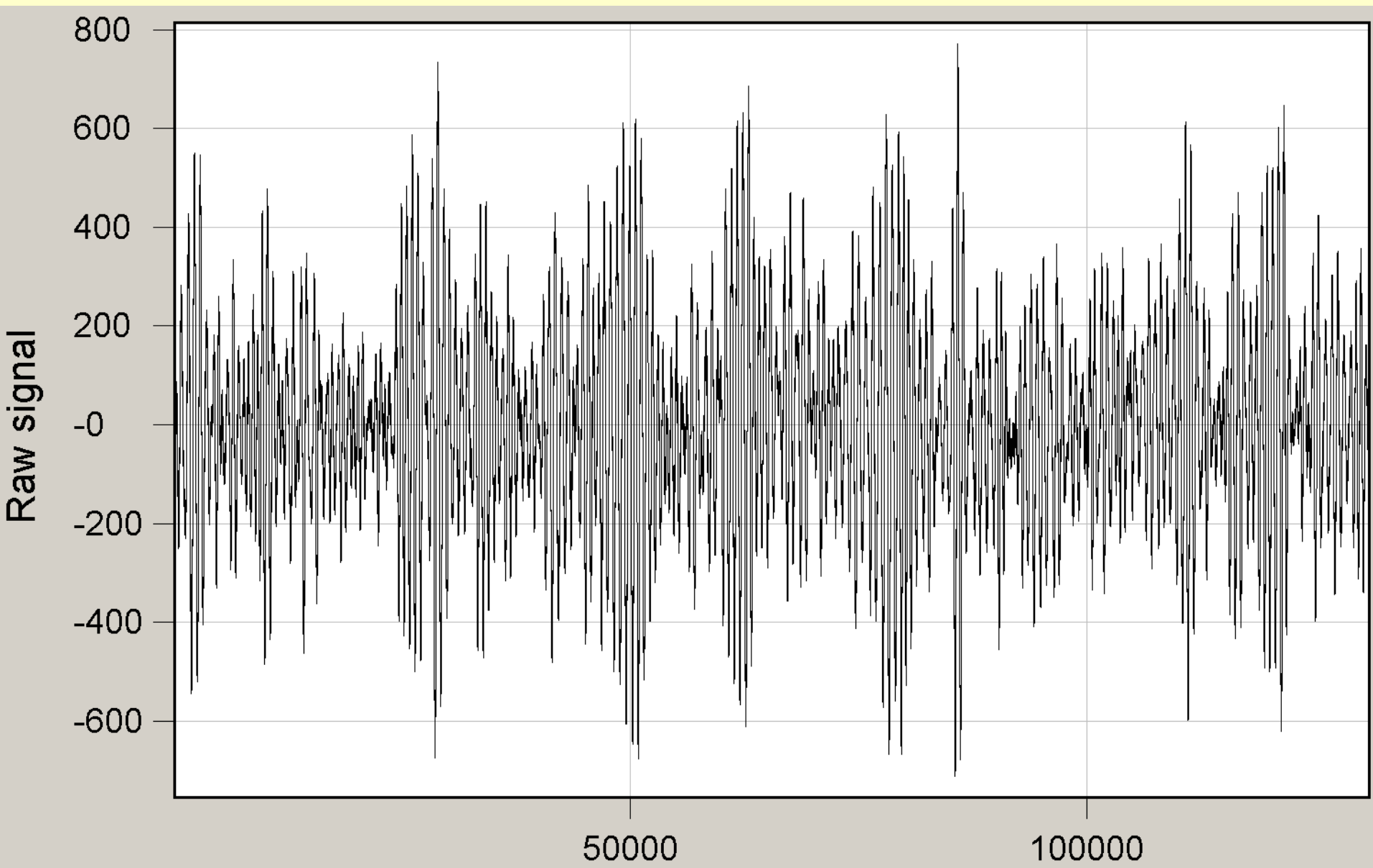
CF Summary

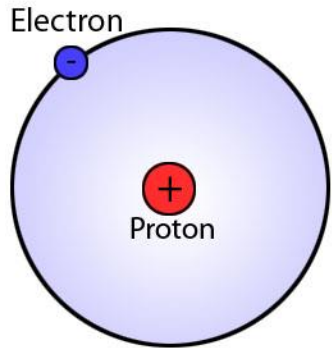
- CF method allows to analyze and visualize nearly periodic processes
- It allows to locate special features in data curves (flip-flops, trends etc)
- Method is of exploratory type and must be supplemented by other techniques.

What is FDC method?







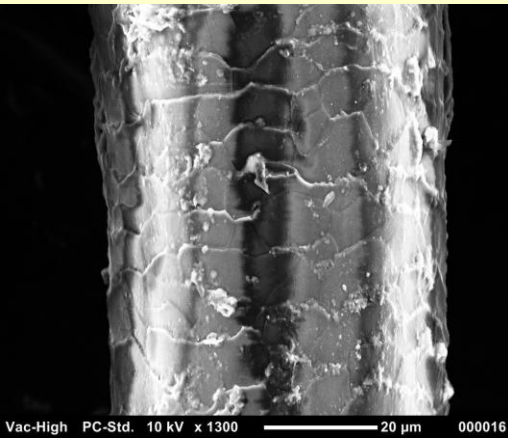


$$\text{LIGO } h = 10^{-21}$$

$$4000 * 10^{-21} = 0.4 * 10^{-17} \text{ m}$$

PROOTONI DIAMEETER $1.67\text{-}1.74 * 10^{-15} \text{ m}$
 JUUKSED $0.17\text{-}1.81 * 10^{-4}$

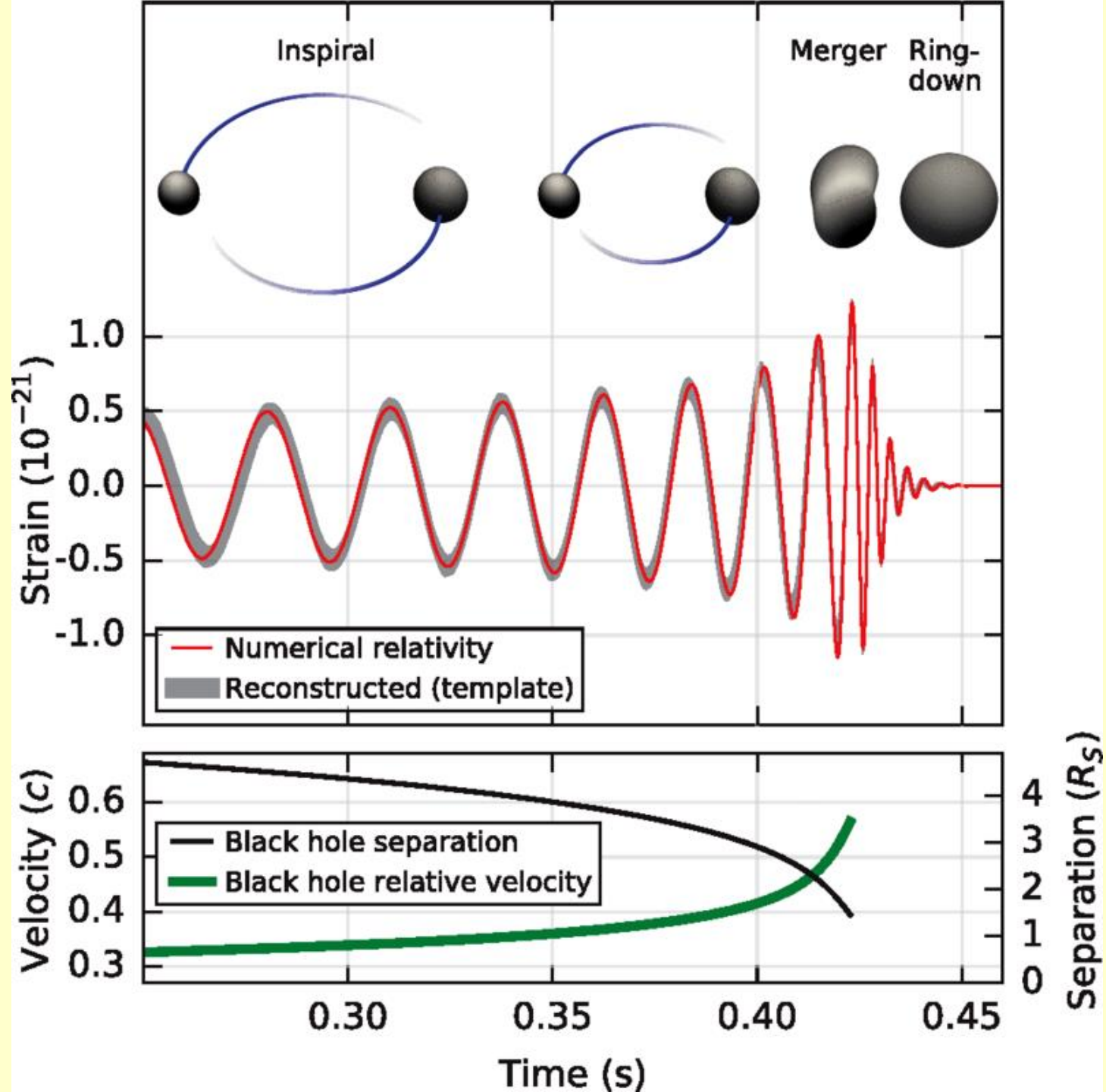
PROOTON/LIGO = 400
 (Mujal 1000-10000)

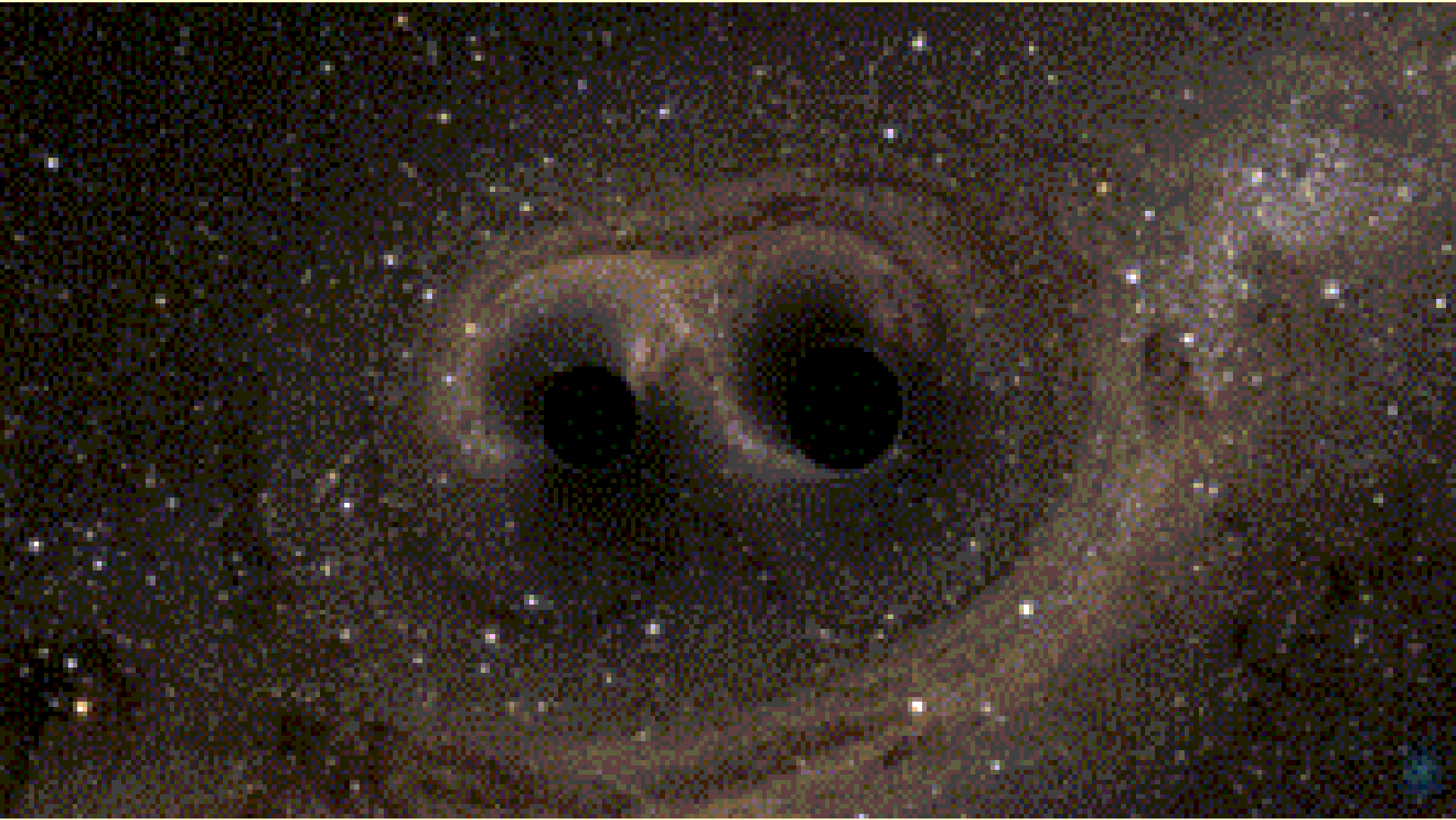


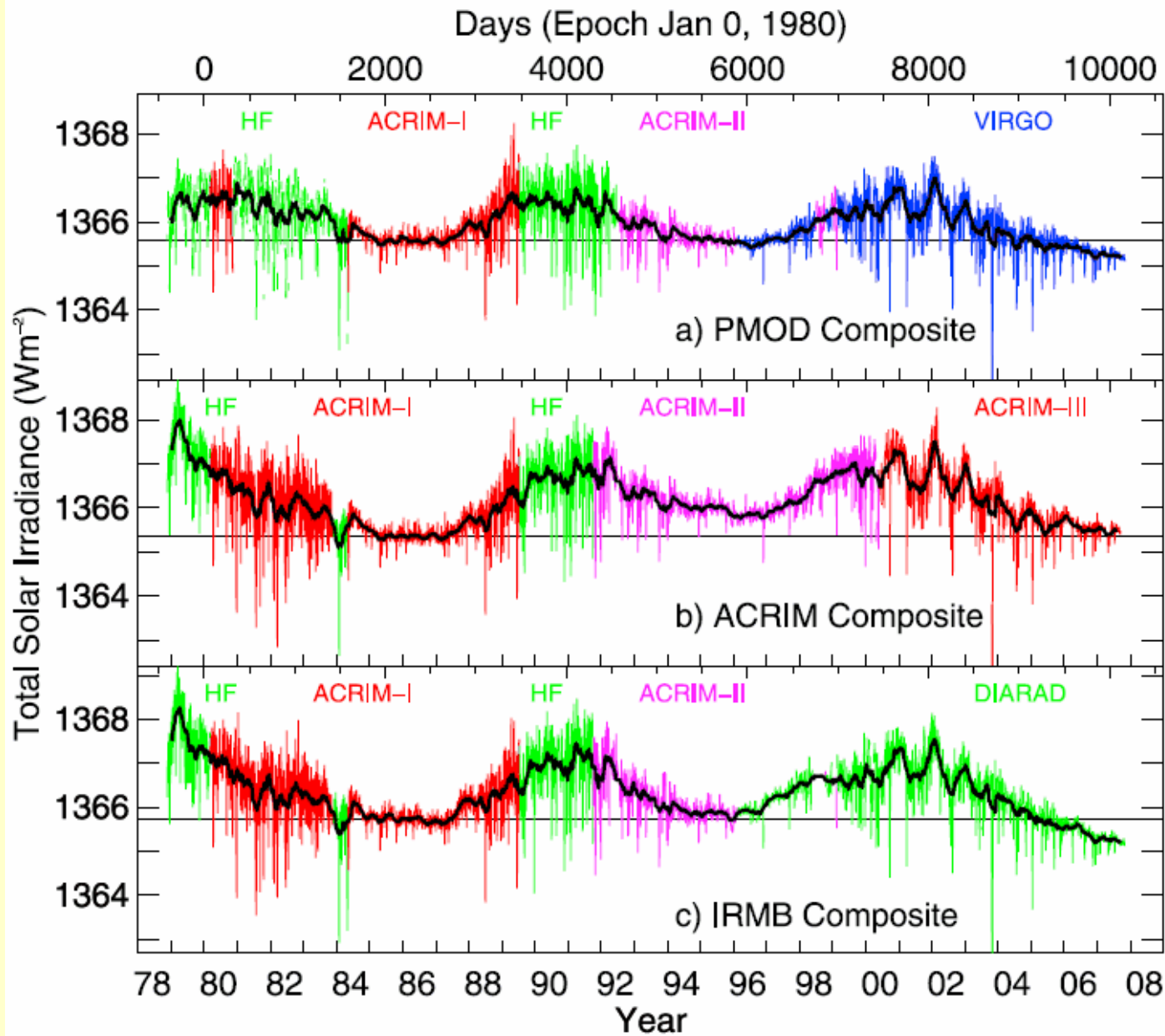
AU $0.15 * 10^{12} * 10^{-21} = 0.15 * 10^{-9} \text{ m}$
 Proxima Centauri $0.4 * 10^{17} * 10^{-21} = 0.4 * 10^{-4}$
 Foonikiirguse tee $0.127 * 10^{27} * 10^{-21} = 127\text{km}$
 Tallinn-Põltsamaa

$$g' = \frac{\Delta g}{d} = \frac{\text{change in gravity}}{\text{displacement}}$$

$$h = \frac{2\Delta d}{d} = 2 \times \frac{\text{change in displacement}}{\text{displacement}}$$

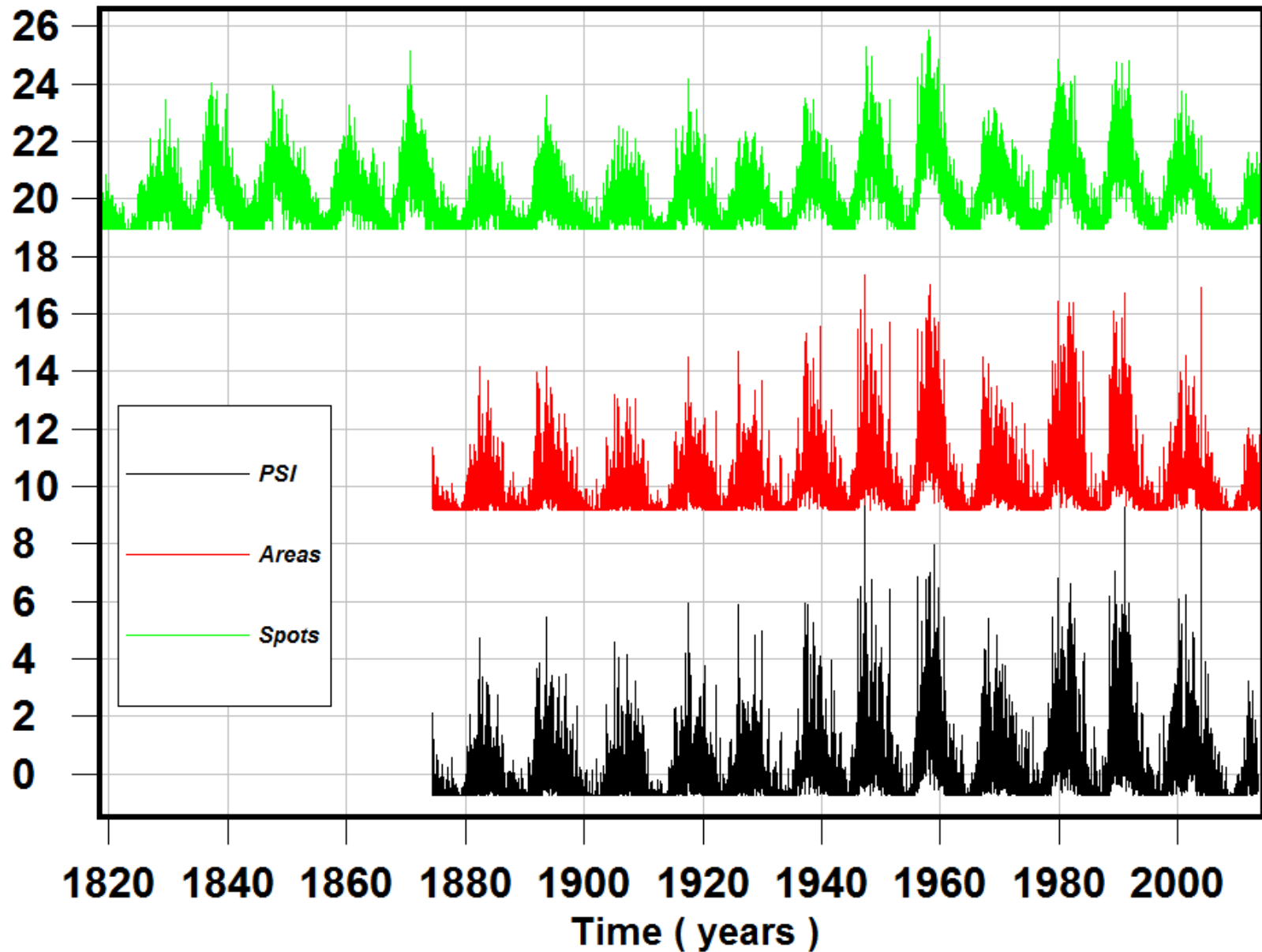






Three targets – TSI Composites

Normalized and shifted



Proxies

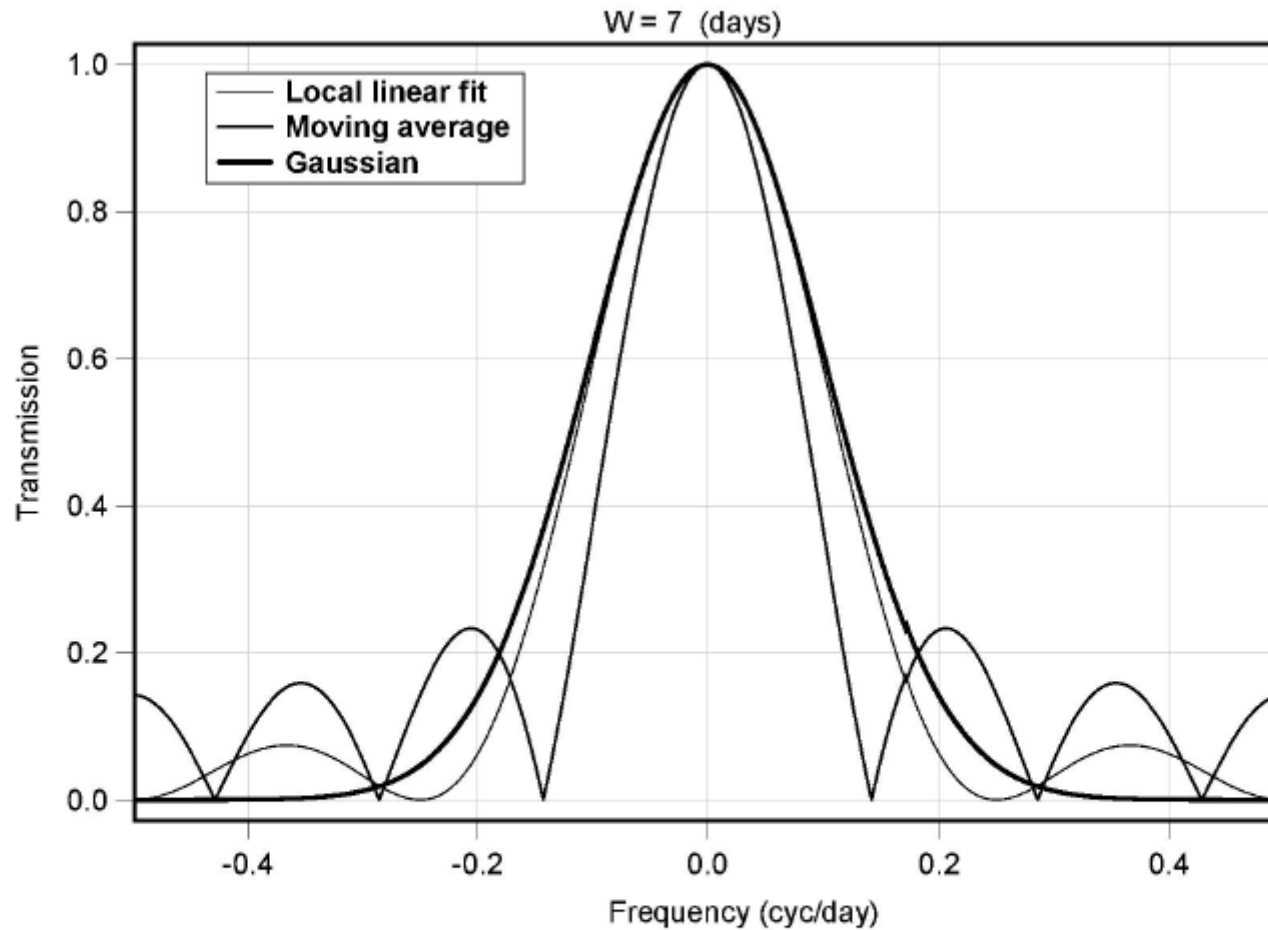


Fig. 1. Three different transmission curves for the specific width of the time domain filter.

$$T(\nu) = \exp^{-(\nu W)^2}$$

Transmission curve for Gaussian filter

Data \rightarrow FFT \rightarrow Multiple by TC \rightarrow FFT⁻¹ = Smoothed data

LF part = smoothed data

HF part = data – smoothed data

To compare different daily data sets we:

A. Cut off parts for which both data exist.

B. Compute $R_c =$

$$\frac{\sum_{i=1}^n (x_i - \bar{x})(y_i - \bar{y})}{\sqrt{\sum_{i=1}^n (x_i - \bar{x})^2} \sqrt{\sum_{i=1}^n (y_i - \bar{y})^2}}$$

	PMOD	RMIB	ACRIM	SATIRE-S
Original				
PMOD	1.0000	0.9322	0.8553	0.8969
RMIB	0.9322	1.0000	0.9167	0.8586
ACRIM	0.8553	0.9167	1.0000	<i>0.8105</i>
SATIRE-S	0.8969	0.8586	<i>0.8105</i>	1.0000
LF				
PMOD	1.0000	0.9191	0.8422	0.9446
RMIB	0.9191	1.0000	0.9022	0.8404
ACRIM	0.8422	0.9022	1.0000	<i>0.7962</i>
SATIRE-S	0.9446	0.8404	<i>0.7962</i>	1.0000
HF				
PMOD	1.0000	0.9391	0.8939	0.8583
RMIB	0.9391	1.0000	0.9424	0.8777
ACRIM	0.8939	0.9424	1.0000	<i>0.8266</i>
SATIRE-S	0.8583	0.8777	<i>0.8266</i>	1.0000

Table 2. Correlation matrices for input target sets.

	PSI	SA	SN	RADIO	MGII	LYMAN
Original						
PSI	1.0000	0.9424	0.8521	0.8722	0.7726	<i>0.7709</i>
SA	0.9424	1.0000	0.8786	0.9041	0.8001	0.8116
SN	0.8521	0.8786	1.0000	0.9466	0.9237	0.9116
RADIO	0.8722	0.9041	0.9466	1.0000	0.9616	0.9552
MGII	0.7726	0.8001	0.9237	0.9616	1.0000	0.9735
LYMAN	<i>0.7709</i>	0.8116	0.9116	0.9552	0.9735	1.0000
LF						
PSI	1.0000	0.9978	0.9890	0.9943	0.9885	0.9896
SA	0.9978	1.0000	0.9880	0.9890	<i>0.9822</i>	0.9822
SN	0.9890	0.9880	1.0000	0.9915	0.9858	0.9841
RADIO	0.9943	0.9890	0.9915	1.0000	0.9968	0.9930
MGII	0.9885	<i>0.9822</i>	0.9858	0.9968	1.0000	0.9900
LYMAN	0.9896	0.9822	0.9841	0.9930	0.9900	1.0000
HF						
PSI	1.0000	0.8939	0.7410	0.8172	0.5715	0.5852
SA	0.8939	1.0000	0.7452	0.8315	<i>0.5527</i>	0.5909
SN	0.7410	0.7452	1.0000	0.8020	0.7054	0.6663
RADIO	0.8172	0.8315	0.8020	1.0000	0.8047	0.8014
MGII	0.5715	<i>0.5527</i>	0.7054	0.8047	1.0000	0.8725
LYMAN	0.5852	0.5909	0.6663	0.8014	0.8725	1.0000

Table 1. Correlation matrices for input proxy data sets.

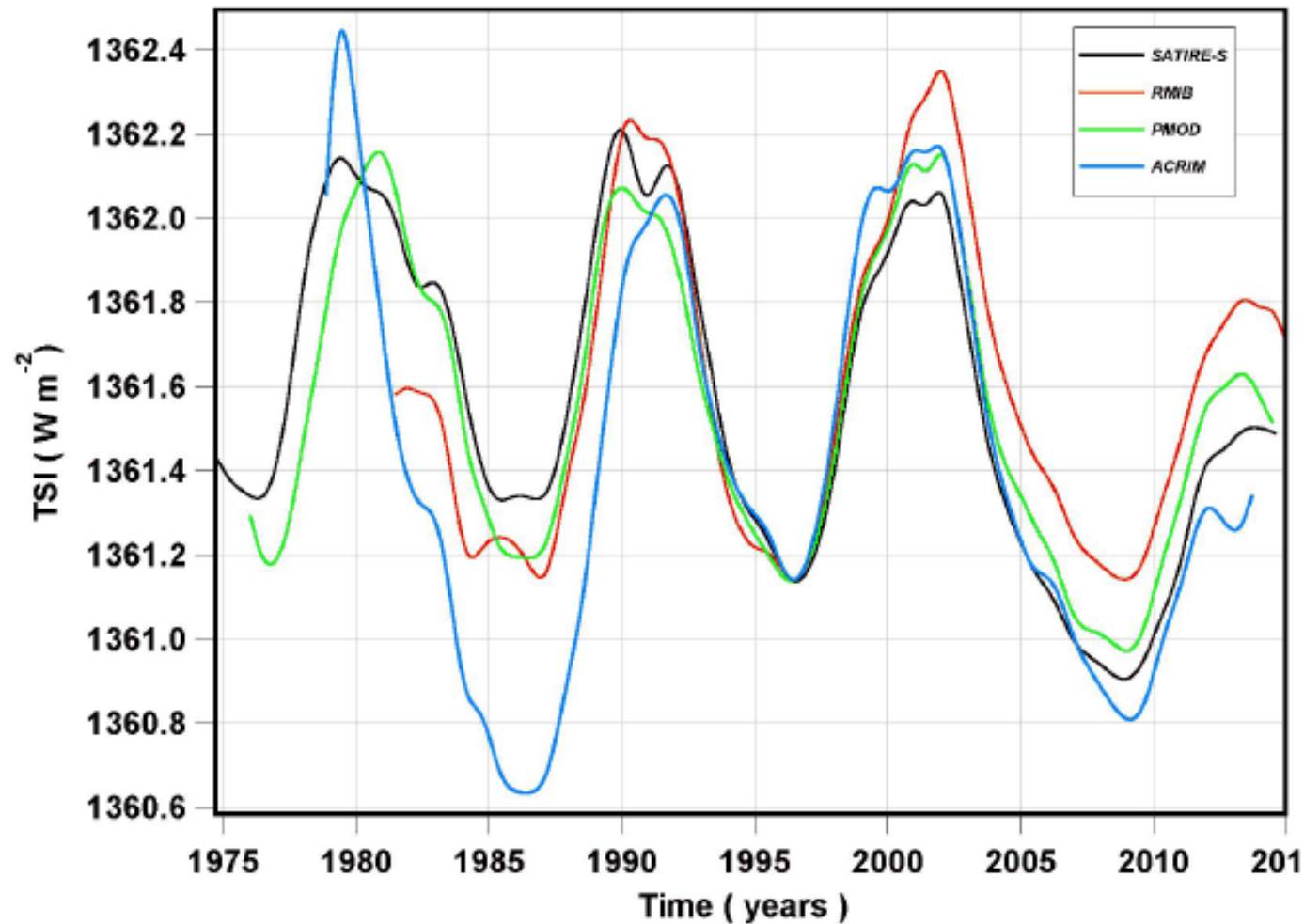
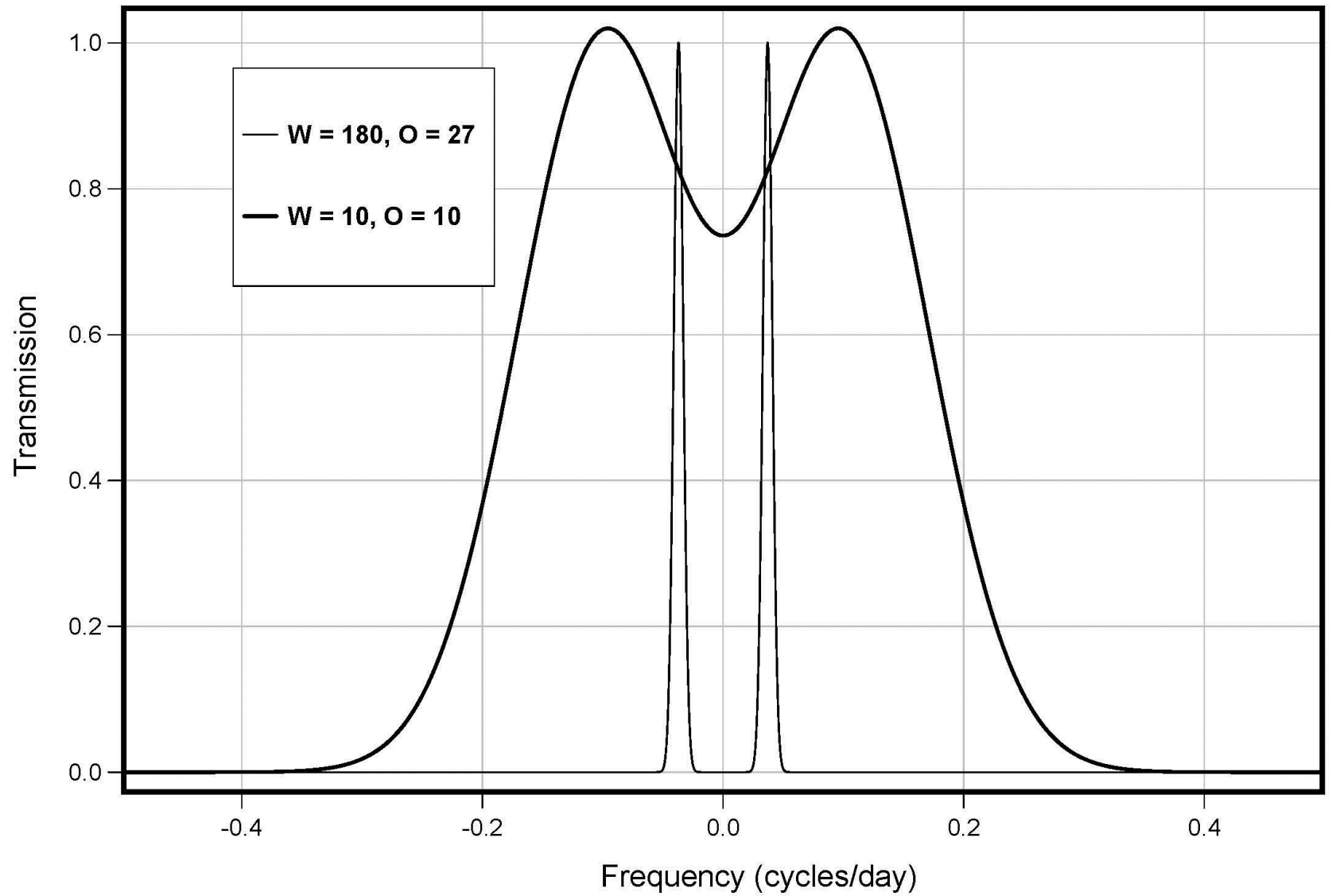
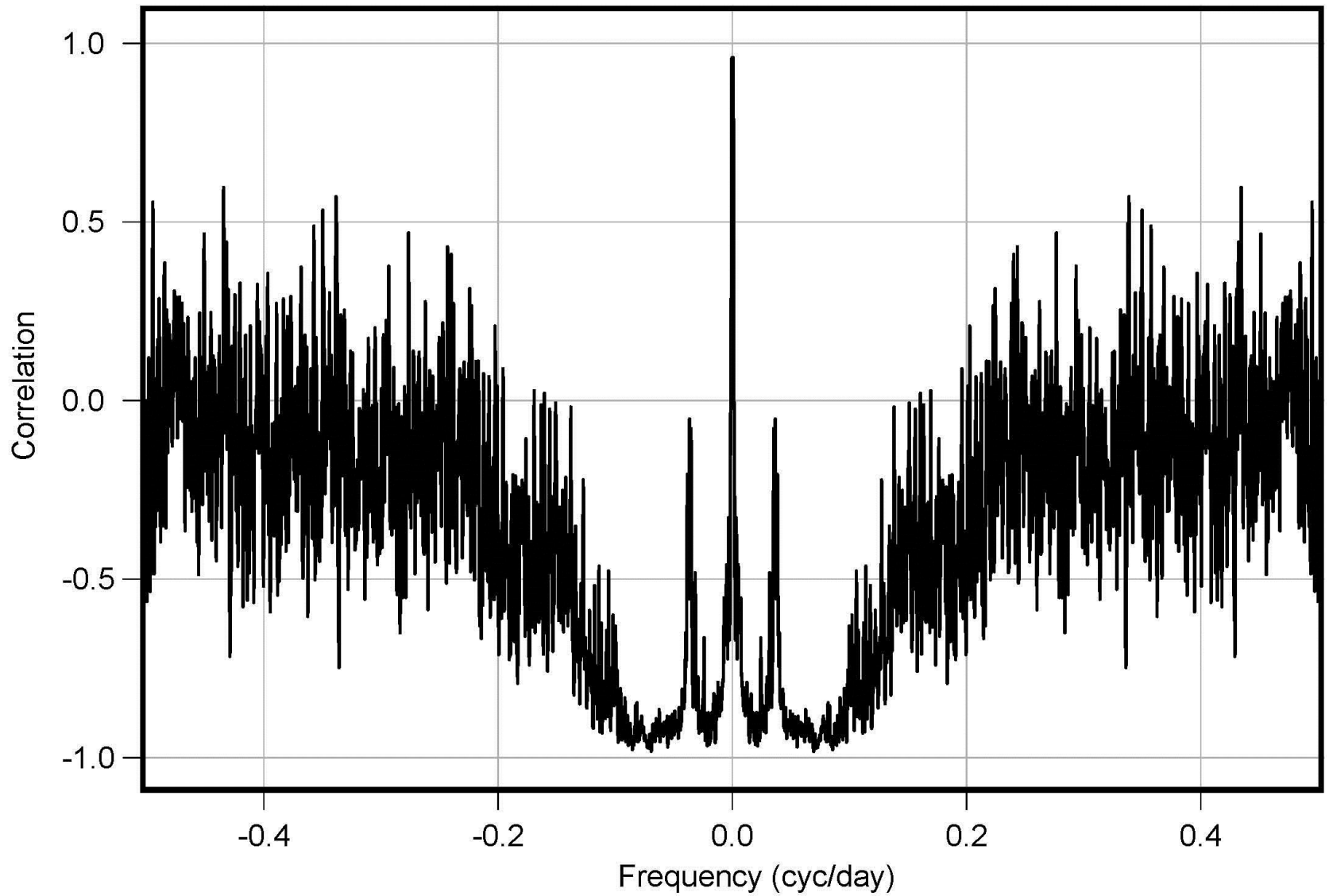


Fig. 6. The major controversy. To recover TSI for the past dates we need current estimates for calibration. But which one to choose? LF parts ($W = 750$ days) of four target TSI composites. The input curves are shifted to common level at 1996.465.

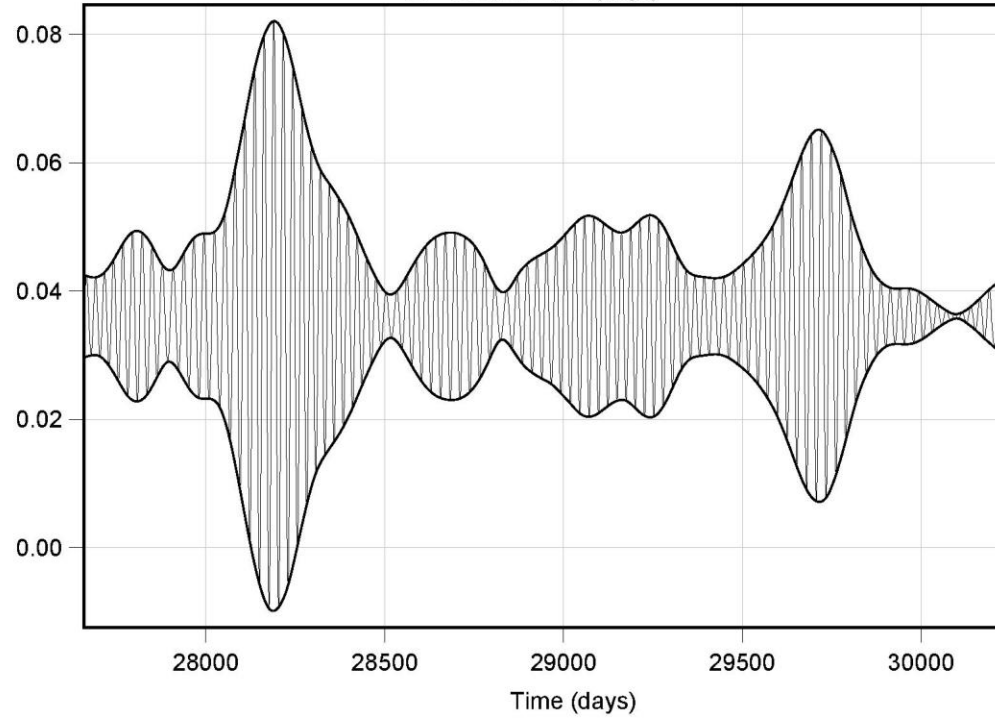


PMOD vs PSI

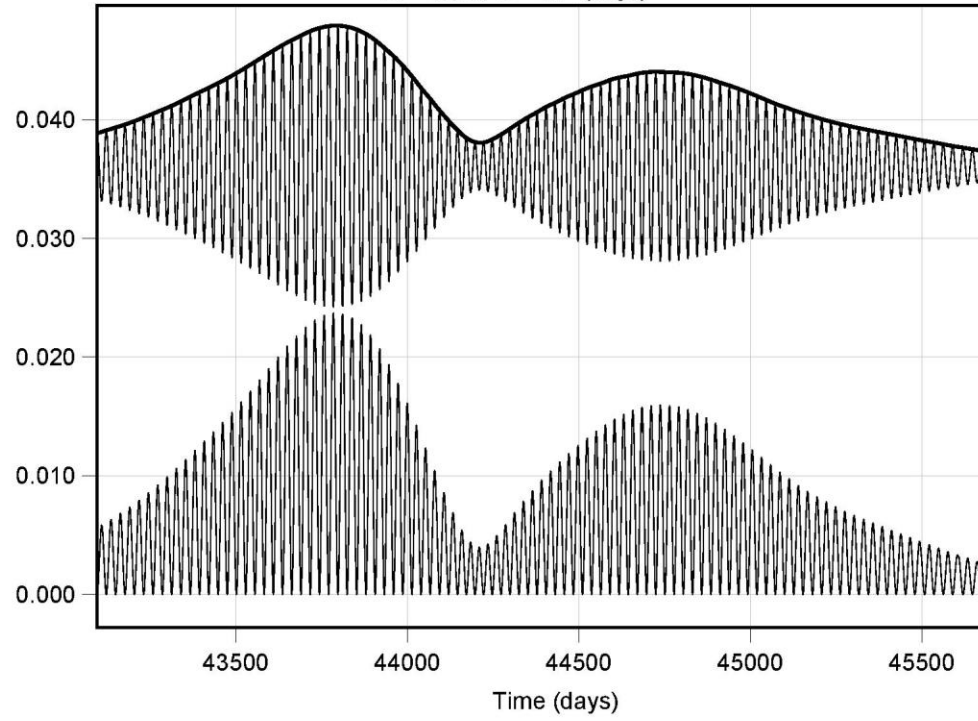


$W = 2000$ days, varying offsets

$W = 300, O = 27$ (days)



$W = 1000, O = 27$ (days)



$$SS = \sum_{i=1}^N (y(t_i) - \sum_{l=0}^L a_l E_l(\dots)[t_i])^2$$

- Start model building from including into it constant level and the input curve as components.
- In each additional step try all the variants from the full library of filtered or otherwise processed components to be as possible next components.
- Evaluate prospective candidates by correlating obtained model with actually observed signal.
- Finally, use the obtained model to hindcast unobserved irradiance values.

Coefficient	Predictor	Value
a_0	1.0	1365.551
a_1	$E(0, 0)$	-8.030
a_2	$E(766.229, 0.0)$	19.049
R_c	0.8597	

Table 4. Summary of least squares fit results with one smoothed component.

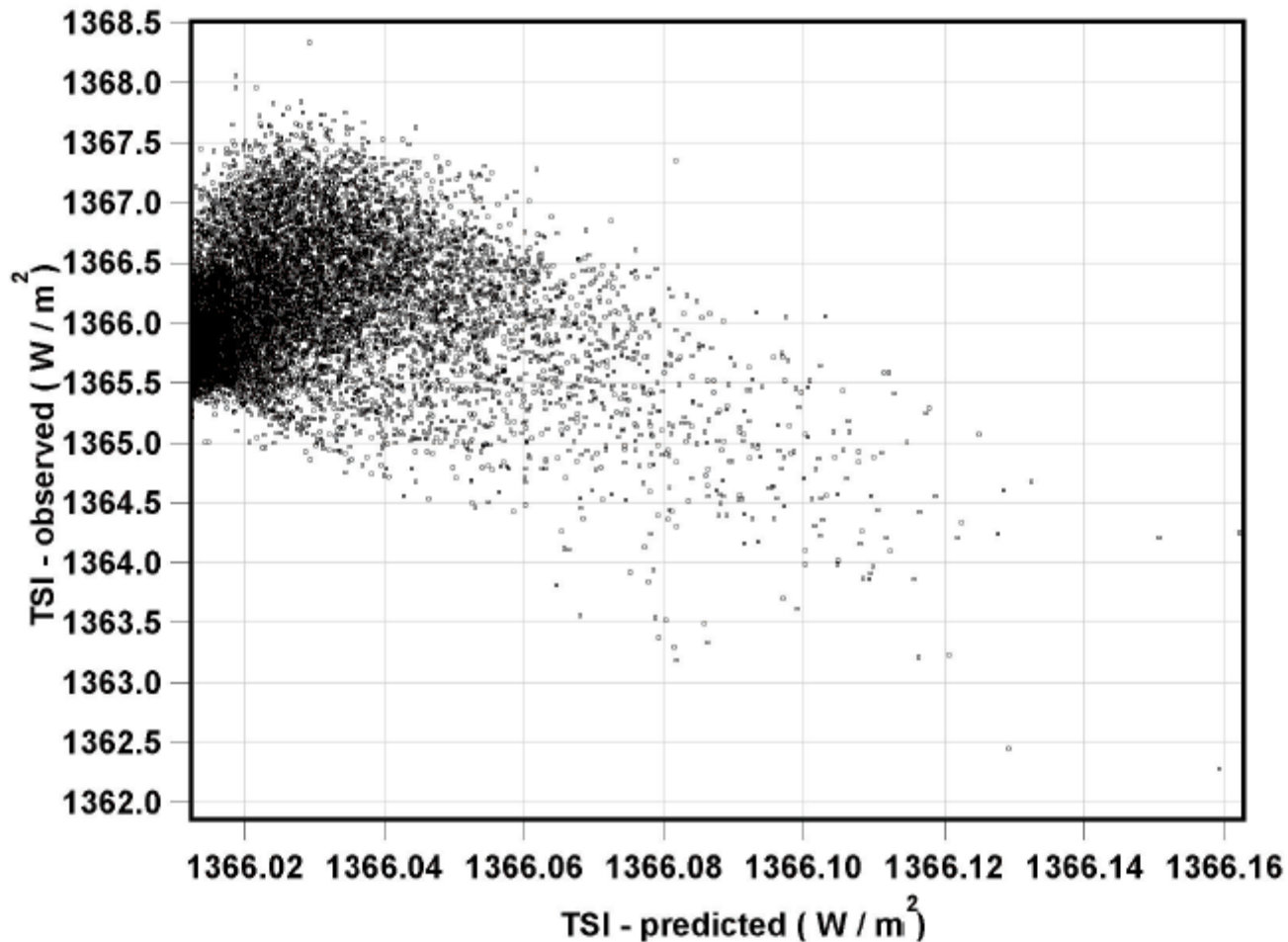


Fig. 7. Common parts of the PMOD and PSI are practically uncorrelated ($R_c = 0.0300$). Here we use predicted-observed crossplot as we will do below for more general than trivial linear regression model.

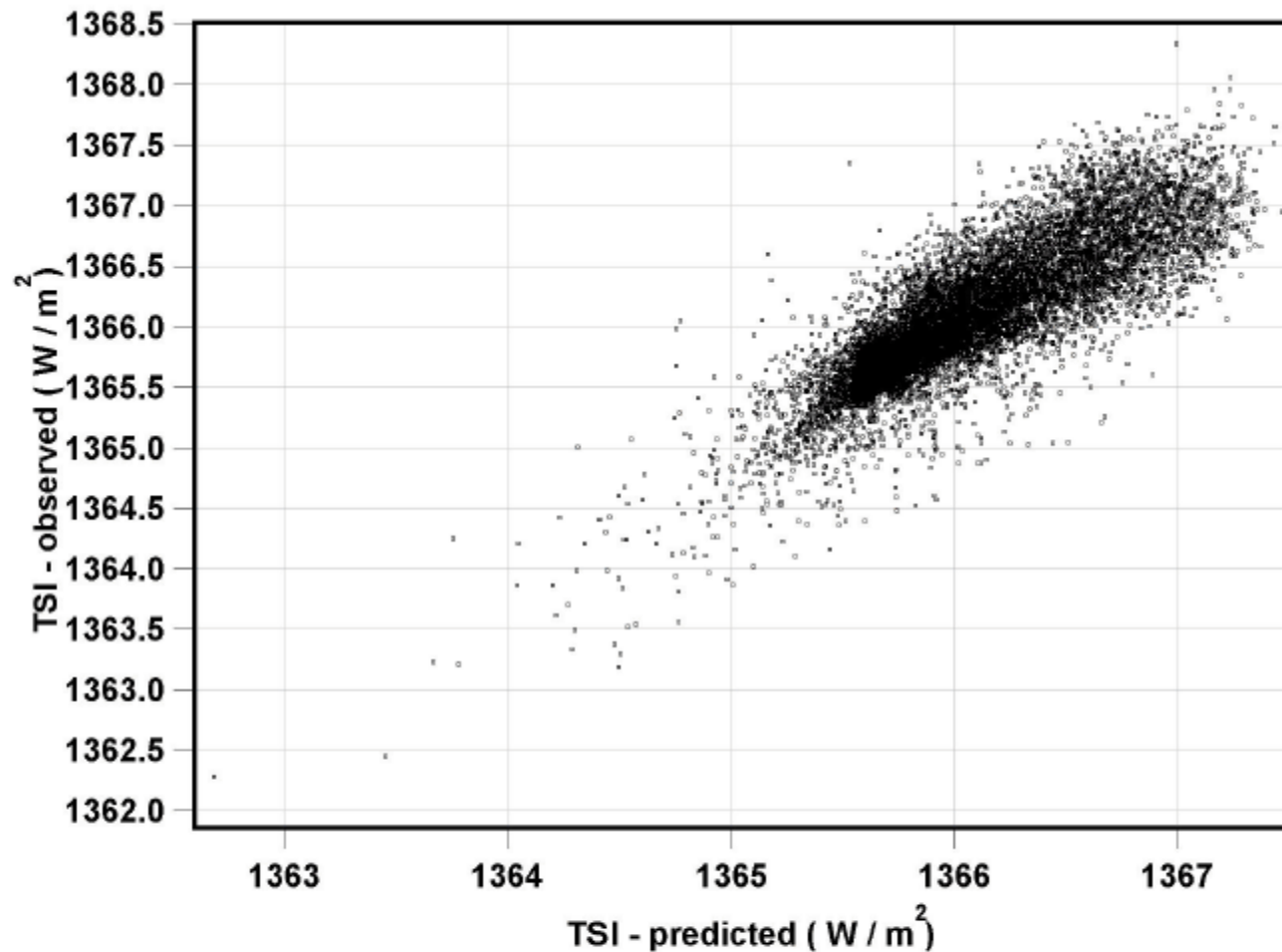


Fig. 9. The observations and simple model with smoothed component is much more strongly correlated ($R_c = 0.8597$).

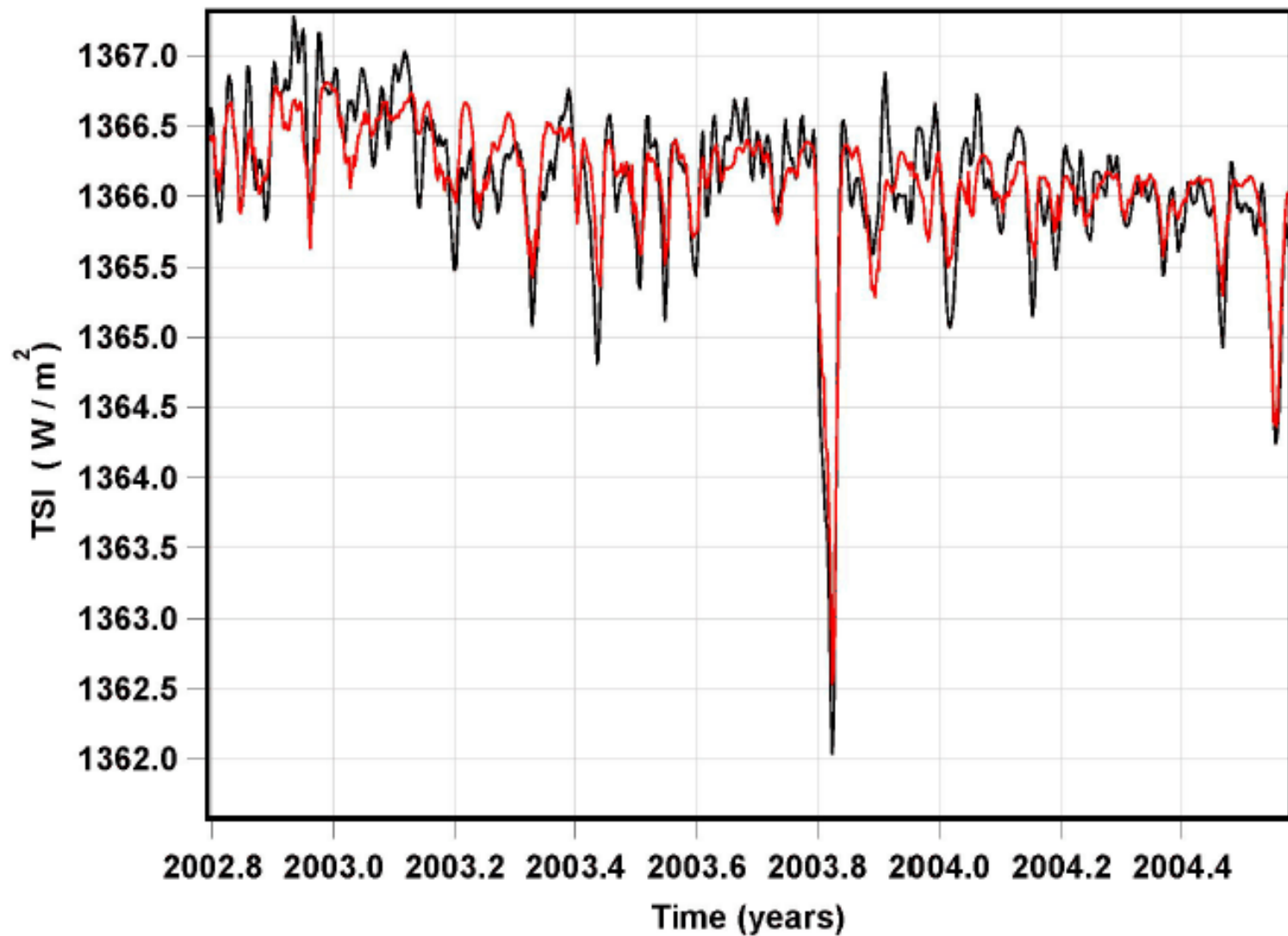


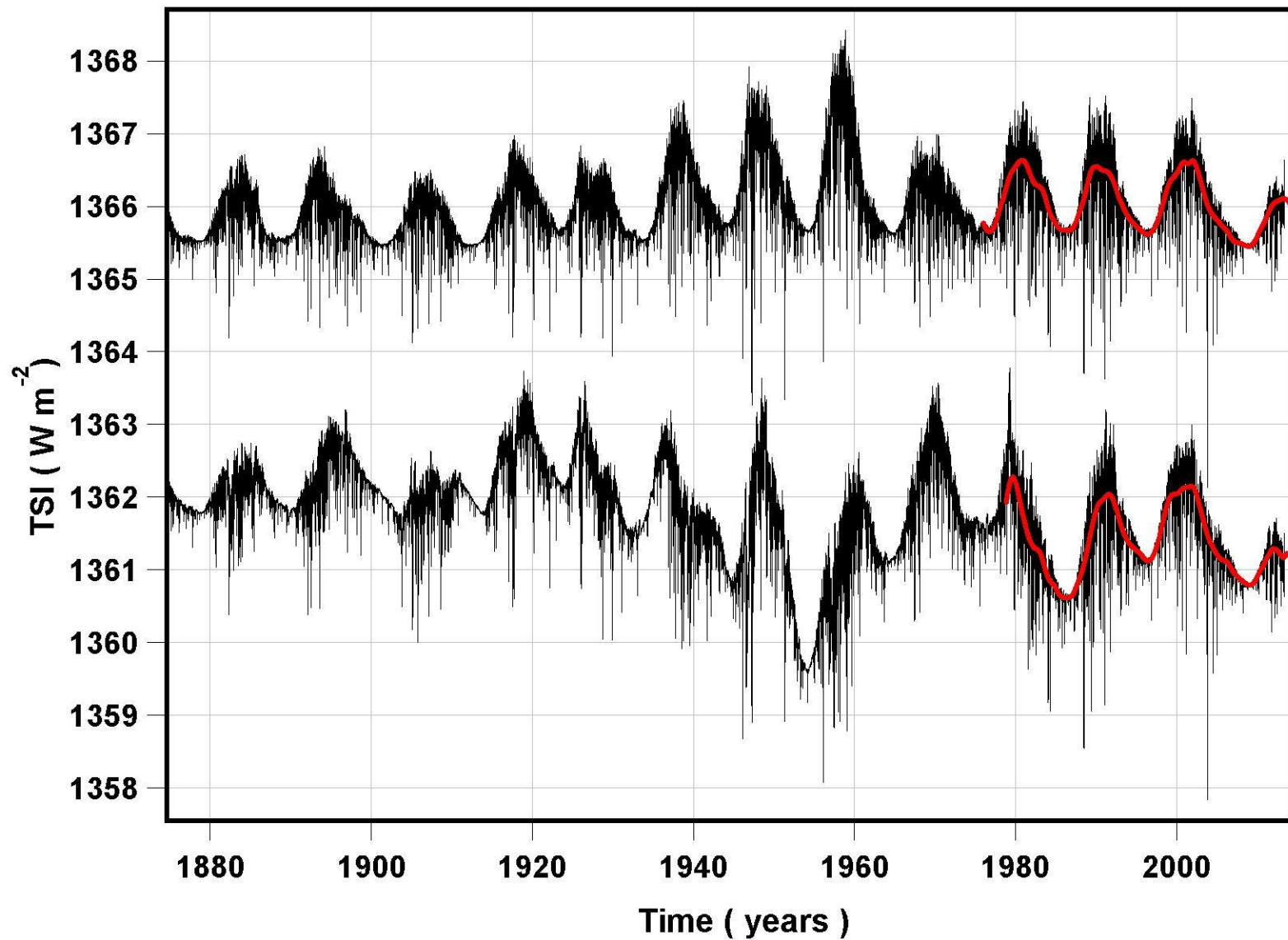
Fig. 10. Reconstruction of the TSI using the HF part of PSI combined with LF part of PMOD. Reconstruction is plotted in red, target in black.

N	Type	Width	1/Offset	R_c
1	E	766.229110	-	0.85973057
2	E_t^+	399.116082	27.103323	0.87599719
3	E^-	2413.855149	1811.476298	0.88710035
4	E	10.083440	10.148801	0.89328020
5	E^-	137.021917	102.081918	0.89713987
6	E^+	3509.347248	12.475225	0.90071914
7	E^+	2474.591733	20.816371	0.90294868
8	E^-	11.057883	10.679024	0.90478582
9	E_t^-	12.699491	11.198220	0.90733729
10	E_t^+	133.649130	188.570202	0.90864964
11	E_t^+	189.738179	198.084112	0.91081665
12	E_t^-	901.197452	28.196168	0.91161825
13	E_t^+	5170.005637	140.675553	0.91222860
14	E_t^+	2544.129259	31.414278	0.91284601
15	E_t^-	33.610573	9.976299	0.91336121

Table 8. Modeling PMOD using PSI data. First 15 components from the greedy search for regression components. Parameters W and O are selected without restrictions.

N	Type	Width	1/Offset	Correlation
1	E_t^+	5170.005661	4419.832453	0.78193389
2	E_t^+	2519.302633	1630.468830	0.83406728
3	E^+	1503.913332	289.744282	0.85372950
4	E^-	3406.542205	148.810590	0.87693631
5	E	362.381918	27.341738	0.88562065
6	E_t^+	430.606068	2183.735031	0.89144597
7	E^-	2340.484301	300.893810	0.89771429
8	E^-	165.079222	93.264999	0.90193772
9	E	9.637961	10.600217	0.90548052
10	E^+	2570.699109	27.380182	0.90766399
11	E_t^+	15.521919	34.876082	0.90919779
12	E^-	1931.046907	289.584617	0.91083821
13	E_t^+	124.463532	112.081094	0.91196667
14	E_t^+	95.268221	105.427923	0.91497974
15	E_t^+	153.399257	109.674353	0.91650578

Table 9. Modeling ACRIM using PSI data. First 15 components from the greedy search for regression components. Parameters W and O are selected without restrictions.



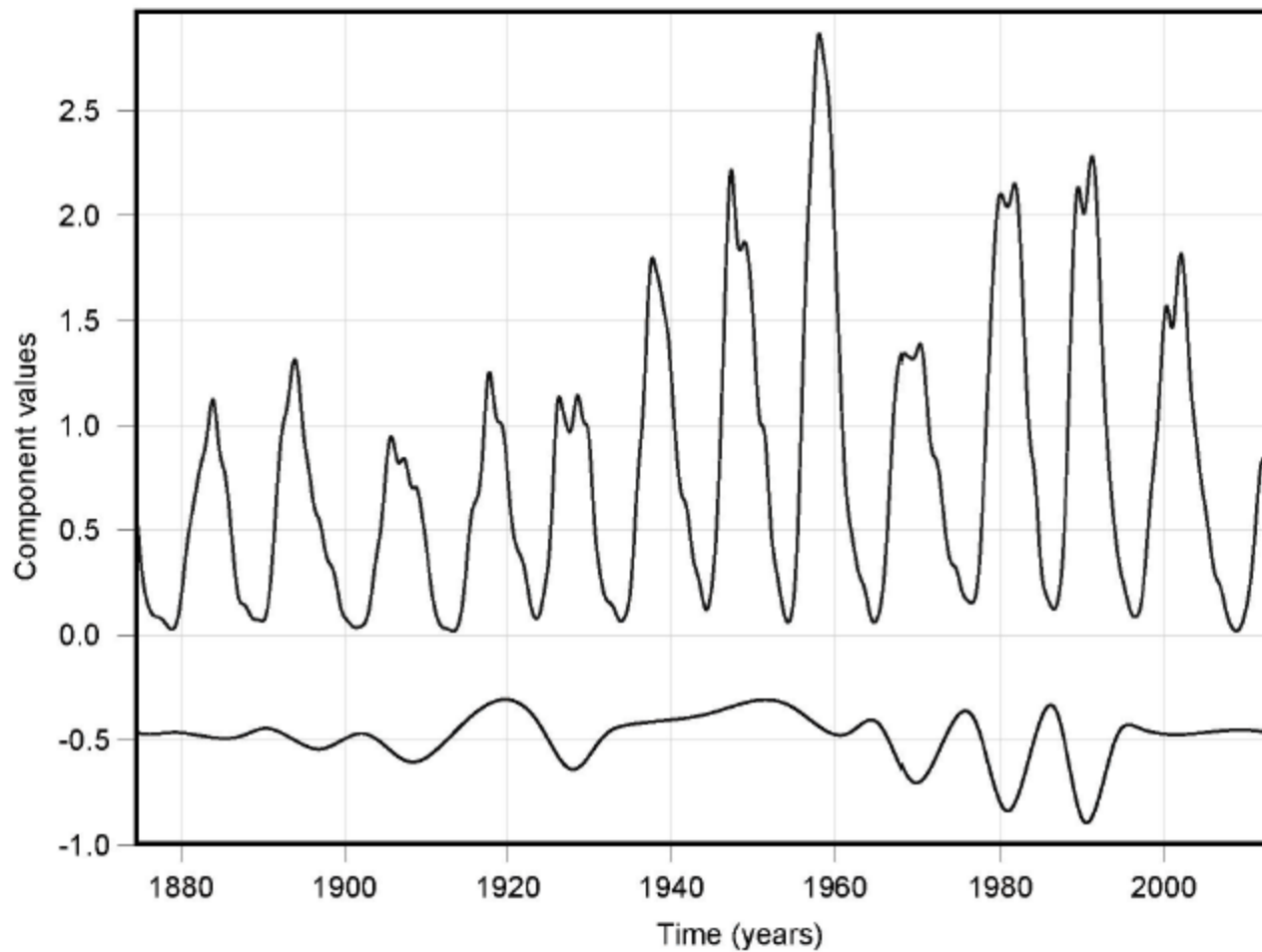


Fig. 14. The first (upper) and third (lower) components of the full scale PSI to PMOD model.

Cross-prediction and sieving

$$R_c = \max_{W,O,M} \min(R_c^{I \rightarrow II}(W, O, M), R_c^{II \rightarrow I}(W, O, M))$$

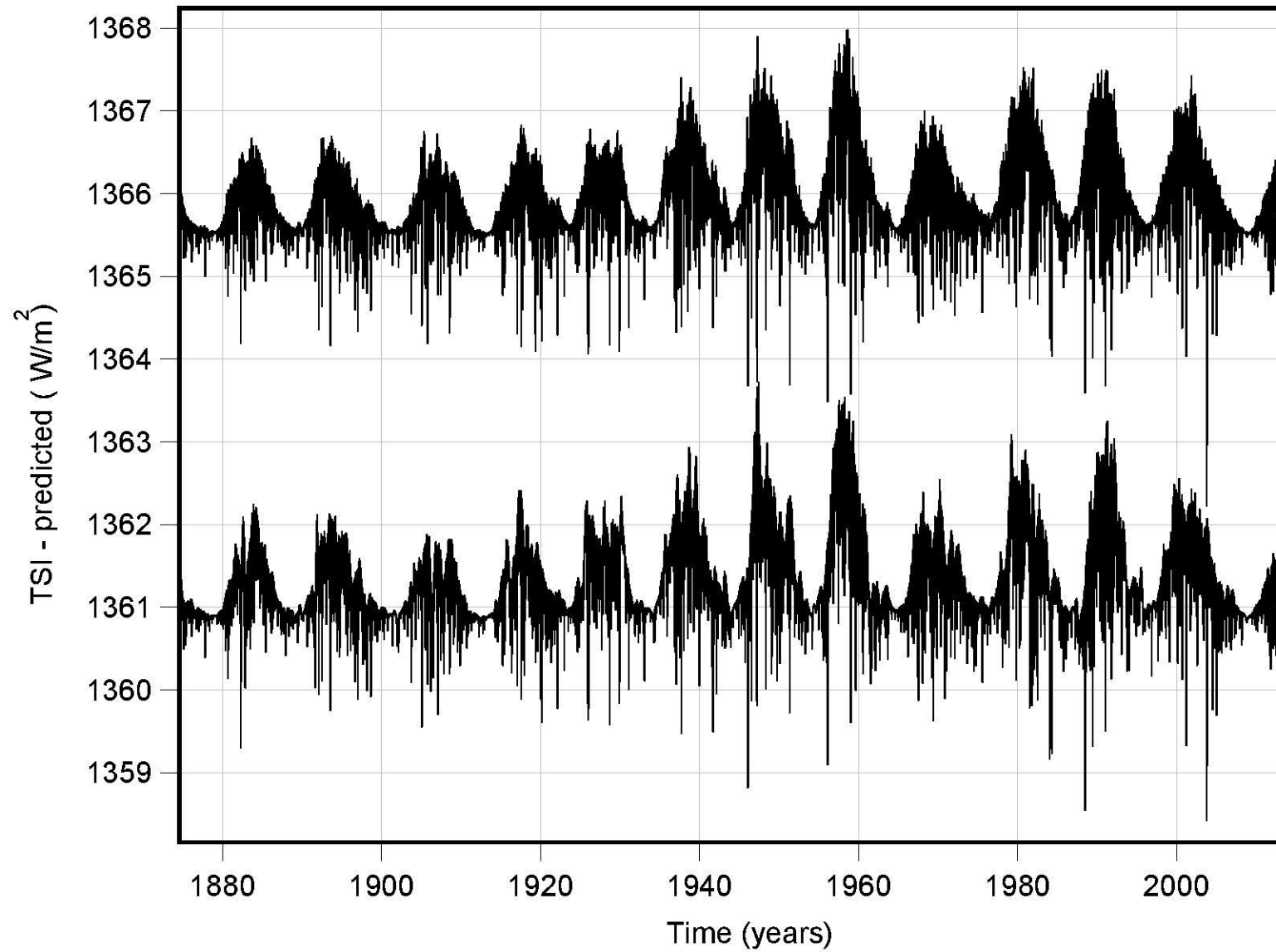
$W < 2000$

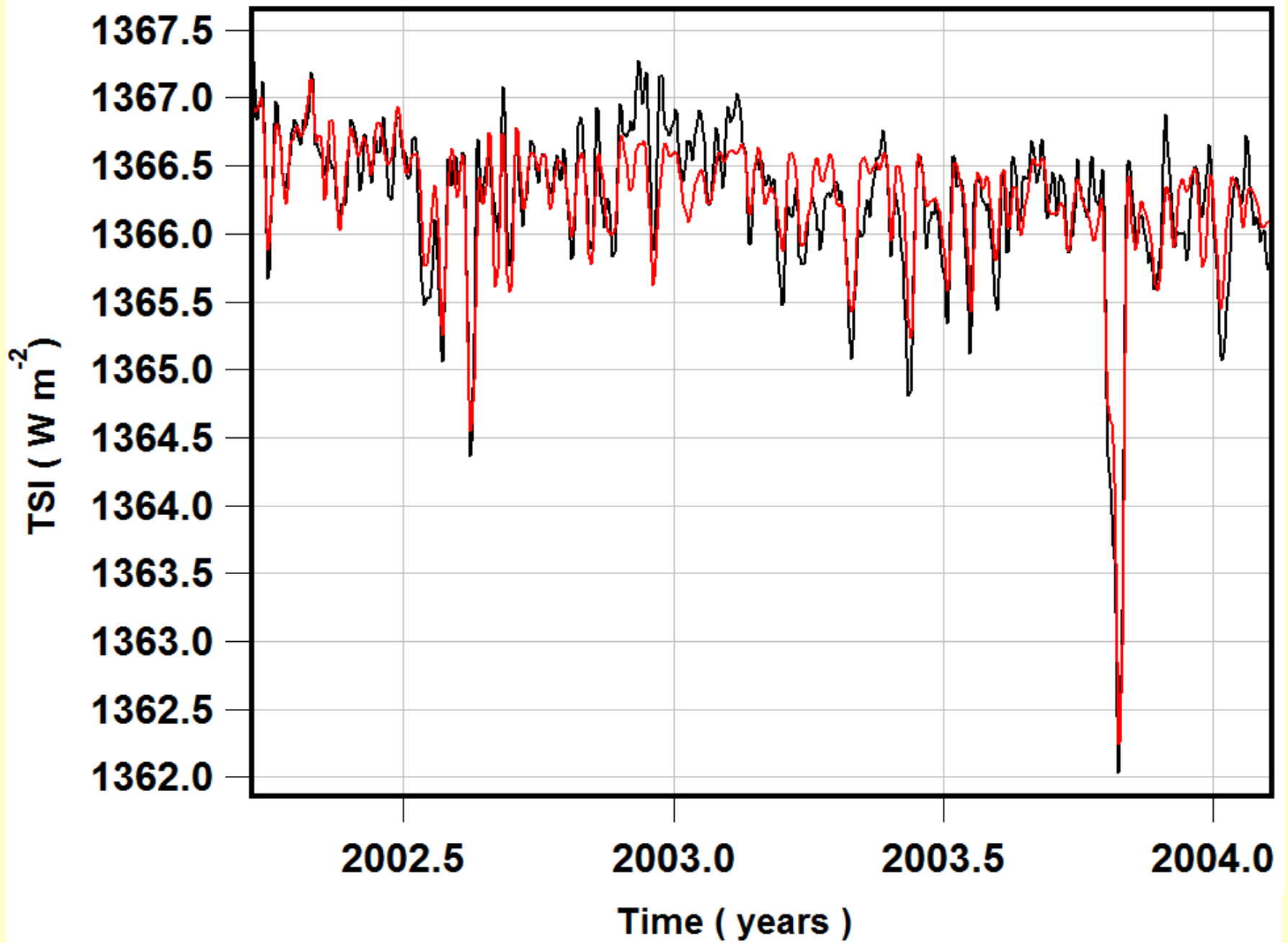
$1/O < 500$

Check for colinearity

Component	Type	Width	1/Offset	Correlation
1	E	766.203360	-	0.85971218
2	E	368.344694	27.205664	0.87183687
3	E	11.076777	10.507722	0.87798356
4	E	510.918696	-	0.87798440
5	E_t^-	126.141442	85.206093	0.88078618
6	E^-	137.407018	9.624734	0.88213771
7	E_t^-	8.636770	8.672939	0.88481412
8	E^+	356.511603	61.922806	0.88584926
9	E	194.211239	8.970496	0.88652112
10	E^+	124.335750	112.065571	0.88693209
11	E_t^+	145.786806	194.401278	0.88695375
12	E^+	145.491923	169.169762	0.88977830
13	E^+	815.678995	82.630138	0.89115533
14	E_t^+	99.363542	89.764059	0.89158876
15	E	173.673683	77.786024	0.89236231

Table 10. Modeling PMOD data using PSI as a proxy. First 15 components of the regression model where all kind of components were allowed.





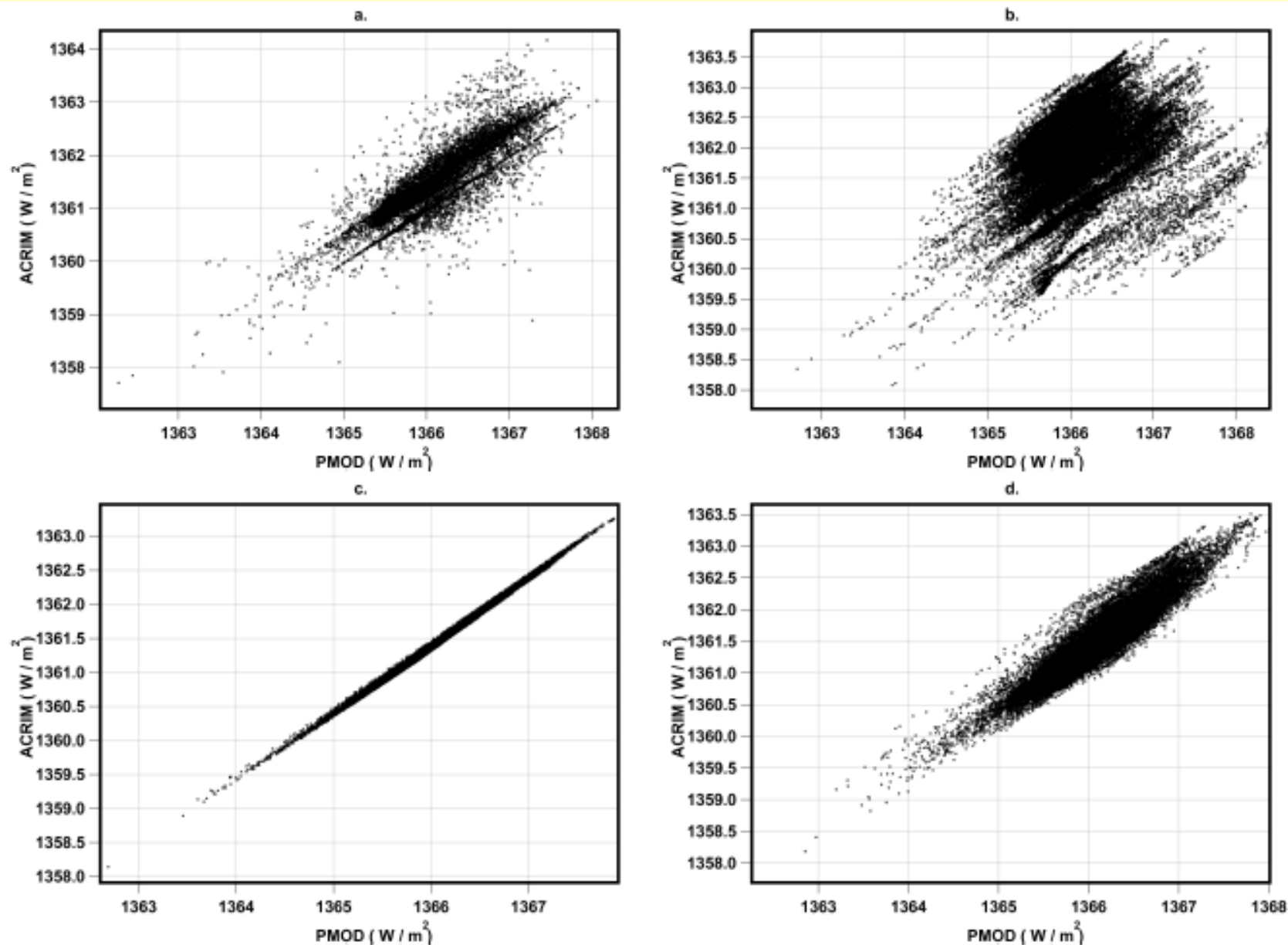


Fig. 10. Correlations between PMOD and ACRIM based predictions. Upper panel: a. crossplot of the original target data sets PMOD versus ACRIM ($R_c = 0.8553$), b. crossplot for solution without restrictions ($R_c = 0.3521$, Fig. II); lower panel: c. crossplot of the predictions based on simplest models ($R_c = 0.9985$), d. crossplot between combined models ($R_c = 0.9384$).

FDC Summary

- The correlations between time series depend on frequency band involved.
- The models based on smoothed, enveloped etc components can be used for prediction, interpolation and stitching of different fragments.
- Current state of affairs with TSI measurement and composite building is very complicated.
- Probably the best data product which can be given to climatologists is nearly primitive model based only on small number of components. It will with high probability correlate with true TSI at the level of $R_c=0.85$ or so.

Final words

- D^2 method - periodicity, multiperiodicity, period stability, coherence length.
- CF method - transients in phase, modulations etc.
- FDC method – filter and correlate!